A Spectrum Sharing Framework for Intelligent Next Generation Wireless Networks

Felipe A. P. de Figueiredo*, Ruben Mennes†, Xianjun Jiao*, Wei Liu*, and Ingrid Moerman*
*Ghent University - imec, IDLab, Department of Information Technology, Ghent, Belgium
†Department of Mathematics and Computer Science, University of Antwerp - iMinds, Antwerp, Belgium
Email: [felipe.pereira, xianjun.jiao, wei.liu, ingrid.moerman]@ugent.be, †ruben.mennes@uantwerpen.be

***Abstract*— The explosive emergence of wireless technologies and standards, covering licensed and unlicensed spectrum bands has triggered the appearance of a huge amount of wireless technologies, with many of them coexisting in the same band. Unfortunately, the wireless spectrum is a scarce resource, and the available frequency bands will not scale with the foreseen demand for new capacity. Certain parts of the spectrum, in particular the license-free ISM bands, are overcrowded, while other parts, mostly licensed bands, may be significantly underutilized. As such, there is a need to introduce more advanced techniques to access and share the wireless medium, either to improve the coordination within a given band, or to explore the possibilities of intelligently using unused spectrum in underutilized (e.g., licensed) bands. Therefore, in this paper, we present an open source SDR-based framework that can be employed to devise disruptive techniques to optimize the sub-optimal use of radio spectrum that exists today. Additionally, we describe three use cases where the proposed framework can be employed along with intelligent algorithms to achieve improved spectrum utilization.**

***Index Terms*— Next Generation Wireless Networks; Cognitive Radios; Collaborative Intelligent Radio Networks; Spectrum Sharing; Coexistence; Experimental Evaluation.**

I. Introduction

The demand for wireless broadband services is insatiable. Current wireless networks can not offer spectrum bandwidth and network capacity to meet the growing traffic demands (e.g., consumers, enterprises, vertical industries, service providers, etc.) forecast for the coming years. According to [1], wireless networks will see an increase in usage by 47 % CAGR by 2021, reaching staggering 49 Exabytes per month, when for example, speeds are expected to reach peaks of 10 Gbps. Additionally, devices ranging from smartphones to wearable fitness recorders to smart kitchen appliances are voraciously competing for bandwidth. With everything considered, around 50 billion wireless devices are expected to be competing for access to wireless communications networks in the next coming years. By 2030, the demand for wireless access is foreseen to be 250 times what it is today [1].

Next generation wireless networks are expected to provide broadband access wherever needed and also support a diversified range of services including everything from self-driving cars to virtual reality, robotic surgery and Internet of things (IoT) [2, 3]. Connections in the order of 1 to dozen of Gbps to vehicles, high speed trains, data-intensive services (e.g., augmented reality, immersive 360° experiences, etc.) are some of the applications which will drive the demand for more coverage and capacity at reduced cost in next generation wireless networks [4]. Unfortunately, the wireless radio spectrum is a scarce resource, and the available wireless bandwidth does not scale with the needed wireless bandwidth [5]. Hence, it is of vital importance for next generation wireless networks to introduce more spectrum efficient wireless technologies for coping with the ever increasing traffic and service demands.

The development of technologies for next generation wireless networks will be driven by three broad use cases families, namely, Enhanced Mobile Broadband (eMBB), Ultra Reliable Low Latency Communications (URLLC), and Massive Machine Type Communications (mMTC). They aim at significantly improving performance, scalability and (cost/energy) efficiency of the current wireless networks such as LTE. These new use cases and their direct requirements will demand huge improvements in comparison with the previous generation of IMT systems [6]. Next, we briefly explain each of of them and list some possible applications [6, 7].

- **eMBB**: this use case will focus on enhancements to the data rate, user density, latency, capacity and coverage of the actual wireless broadband access networks [8]. Some applications of this use case are: (a) High-speed mobile broadband; (b) Augmented Reality; (c) Virtual Reality; (d) Smart office environment, i.e. all devices wirelessly connected; (e) Pervasive video, e.g., high resolution video communications, ultra high definition multimedia streaming,etc.
- **URLLC**: it will allow devices and machines the possibility to communicate with ultra-reliability, high availability and very low latency, which makes it ideal for the following applications [9]: (a) Wireless Industrial Control; (b) Factory Automation; (c) Remote Surgery; (d) Cellular Vehicle-to-Everything (C-V2X) communications; (e) Drone communications; (f) Smart Grids; (g) Public Safety.
- **mMTC**: it will focus on enabling communications between devices that are low-cost, massive in number and battery-driven [7, 8]. This use case is intended to support applications like: (a) Smart metering; (b) Smart Cities; (c) Asset tracking; (d) Remote monitoring, e.g., field and body sensors.

In consequence of these new use cases, the next generation of wireless networks will be required to deliver ultra-fast

Preprints (www.preprints.org) | NOT PEER-REVIEWED | Posted: 1 October 2018 doi:10.20944/preprints201810.0017.v1

speeds, low latency, huge coverage and excellent reliability to dozen of billions of wireless devices. It is worth mentioning that not all of these requirements have to be met at the same time, as different services have different subsets of QoS requirements. Additionally, different services with different QoS constraints further have to share the same spectrum band

Some approaches that can be used to cope with traffic increase are: (i) increased/improved spectrum availability (such as introduction of new spectrum bands or more efficient/intelligent use of the available ones) [10]; (ii) introduction of technical enhancements (such as new radio interfaces, codecs, use of multicast transmissions, reduction of energy consumption, etc.); (iii) new network structures and topologies (it is achieved by increasing the network density, where more radio sites are added and cell sizes are shrunk) [11]; (iv) traffic offloading to less occupied spectrum bands (offloading traffic onto unlicensed bands makes capacity available for other users in the license band and improves user experience for devices being served in the unlicensed band. It could also happen within unlicensed bands, e.g., offloading traffic from 2.4 GHz to 5 GHz band) [12].

A. *Motivation*

Most of today's channel allocations separate wireless systems by splitting the spectrum into fixed and exclusively licensed bands that are assigned over large and geographically defined regions. This approach restricts access to the spectrum in exchange for guaranteed interference-free communications. These allocations of spectrum are human-driven and not adaptive to the dynamics of the traffic demand and supply. At any given time, many allocated spectrum bands are unused by their licensees while other bands are completely flooded. For example, a report from the Federal Communications Commission's (FCC) Spectrum Policy Task Force (SPTF) shows that 85 % of current allocated radio frequency bands are either partially or completely unused at different times across geographical areas [13]. This kind of channel allocation scheme leads to a tremendous waste the spectrum capacity and creates unnecessary scarcity [5].

Spectrum sharing, where more than one user shares the spectrum band, either in time and/or space, is one possible and highly viable approach to achieve better spectrum utilization (i.e., combat spectrum bandwidth scarcity) and meet the foreseen increase in traffic demand. Additionally, spectrum sharing can be categorized into two different types: (i) sharing in unlicensed bands; and (ii) sharing in licensed bands. Type (i) can be further split into spectrum sharing in unlicensed bands (i-A) with and (i-B) without an anchor in licensed bands. Some technologies using sharing type (i-A) are LTE-Licensed Assisted Access (LTE-LAA) and LTE-Unlicensed (LTE-U). LTE-LAA and LTE-U occupies licensed and unlicensed bands at the same time through the use of carrier aggregation. Signalling and traffic with specific Quality-of-Services (QoS) requirements will use licensed bands, while less critical traffic is offloaded to unlicensed bands [12, 15, 16]. Some technologies employing sharing type (i-B) are Wi-Fi and MulteFire, which is a LTE-LAA based technology that works solely in unlicensed bands without the need for an anchor in licensed band [17]. In (i), simple sense-and-avoid techniques such as Listen Before Talking (LBT) and Carrier Sense Adaptive Transmission (CSAT) are applied, to comply with regulations [10]. The need for LBT is mandatory in some regions (e.g., Europe and Japan), and not mandatory in other regions (e.g., US and China) [12]. In (ii), the techniques employed are Spectrum Access Systems (SAS) in the US and Licensed Shared Access (LSA) in Europe. These techniques will be used to allow unused spectrum bands of incumbents to be shared with licensees. Such networks will not use LBT schemes, but will rely on a central licensing authority to ensure that interference is avoided (by setting exclusion/protection zones). Access to shared, licensed-shared and unlicensed spectrum bands will be of huge importance to next generation wireless networks as they have the potential to provide significant gains, both in terms of spectrum efficiency and spectrum reuse that translate to higher data speeds for the users, and enabling new capabilities such as prioritized guaranteed resources (i.e., guaranteed time/frequency resources that provide each network with QoS similar to that it would get from licensed spectrum) and new deployment scenarios [14].

Technologies devised for spectrum sharing in unlicensed bands, such as LTE-U, LTE-LAA and MulteFire avoid interfering with neighbour networks by employing simple sense-and-avoid techniques [15], however, in the foreseen dense and diverse future use of spectrum, these simple schemes will not survive, because only local information about the medium availability and naive avoidance mechanisms are insufficient to maintain end-to-end QoS of multiple competing wireless links. On the other hand, technologies for spectrum sharing in licensed bands such as SAS and LSA avoid interference by having a central arbitrator to decide how the licensees will access the incumbents' band, however, in order to ensure reliable QoS to incumbents and licensees, these technologies can not depend exclusively on geo-location and spectrum data bases to decide how they grant access the spectrum [18]. These licensed-sharing technologies need algorithms that provide fair and demand-driven allocation of spectrum resources to licensees so that incumbents and licensees have their QoS requirements met.

Consequently, in order to reap the full capacity out of available spectrum bands (i.e., licensed, unlicensed or licensed-shared bands) and attain stable and adequate communications links, technologies for the next generation of wireless networks have to go beyond simple interference avoidance, frequency isolation schemes (i.e., fixed channel allocations) and geo-location/data base based access approaches. Next generation radios have to employ greater intelligence and collaboration to avoid interference while maximizing spectrum usage and capacity. These radios will need to intelligently collaborate with their peers in order to manage and optimize use of the spectrum without prior knowledge of each other's operating characteristics [19]. Collaborative intelligent radios should be capable of collaborating with other previously unknown

Preprints (www.preprints.org) | NOT PEER-REVIEWED | Posted: 1 October 2018 doi:10.20944/preprints201810.0017.v1

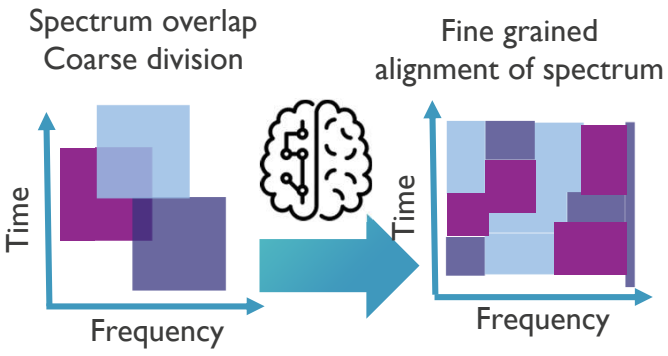

Fig. 1. Collaborative intelligent spectrum sharing.

radios and adapt their communication schemes to optimize the aggregate wireless spectrum usage across all radios, i.e., the ensemble. In other words, next generation wireless networks have to add advanced intelligent algorithms to their radios so that they can collectively develop strategies that optimize use of the wireless spectrum in ways not possible with today's intrinsically simple and often centralized approaches. Figure 1 shows an example of the intelligent collaboration among radios. By applying an intelligent collaborative spectrum sharing scheme, the radios can go from a coarse and often overlapping spectrum distribution (i.e., poor spectrum usage due to the absence of cooperation among radios) to a more fine-grained and aligned spectrum allocation (i.e., optimized spectrum usage). Therefore, the problem that needs to be solved is an extremely complex system involving a high density of heterogeneous wireless devices and technologies competing for the same (and already) scarce spectral resources and serving applications with diverging and dynamic QoS requirements. Such a complex system has a huge parameter space and configuration options, and cannot be solved anymore by simple rules and algorithms based on domain expertise only.

Radios for next generation wireless networks have to be devised not only to communicate reliably in congested and contested environments but also to share radio spectrum without central coordination or spectrum pre-allocation planning across a wide range of heterogeneous radios. Researchers need to rethink the strategies for spectrum access and develop new wireless paradigms where radio networks can autonomously collaborate, understand the current state of the spectrum, and reason how to share the spectrum bandwidth, avoid causing interference and being interfered with, and jointly exploit opportunities to attain the optimum usage efficiency of the available spectrum bandwidth.

Therefore, improved spectrum sharing in unlicensed and licensed bands will drive the research and development efforts towards novel concepts, covering a wide range of topics, including the application of machine learning (ML) and artificial intelligence (AI) algorithms and models to the problem, deployment models, dynamic spectrum allocation and regulatory aspects, radio access design, support of of standalone mode (i.e., standalone operation of access points without mobile infrastructure support), network architectures, ecosystems and business models to fully and intelligently increase the spectrum usage efficiency and enhance coexistence [20].

In recent years, prototyping and experimental validation of innovative wireless technologies has gained importance due to the ever increasing complexity of the wireless ecosystem in emerging next generation wireless scenarios. Such complex system cannot be analyzed anymore with theoretical models or in simulators without applying oversimplified mathematical models and assumptions, far away from limitations imposed by real hardware and real-life environments. Testbeds play a major role in developing and testing new wireless communications technologies and systems and, as with any disruptive technology, prototyping using realistic testbeds is the best way to truly understand the performance trade-offs and limitations. Based on that, several research initiatives are proposing the design of flexible, reconfigurable and reprogrammable prototyping frameworks and platforms for evaluating, comparing and validating the performance trade-offs of innovative wireless devices, communication techniques, network models, services, etc. in realistic testbed environments.

Software Defined Radios (SDRs) [21, 22] are radio communication systems where transceiver components that are typically implemented in hardware (e.g., filters, modulators, demodulators, etc.) are instead implemented in software on a personal computer or embedded system. SDR platforms provide flexibility in reconfiguration of baseband algorithms, software and reprogramming of Radio Frequency (RF) parameters. Moreover, the concept of SDR is very encouraging for the development of novel wireless communications technologies, as software programming allows much faster development cycles and real-life experiments to be conducted for example at local or remote testbeds.

In order to ensure that the next generation of wireless networks can get the most out of collaborative and intelligent spectrum sharing techniques in real-world environments, we present in this paper an open source and runtime configurable SDR-based framework which is suitable for researching and prototyping novel spectrum sharing and coexistence mechanisms in realistic environments [23]. The framework is composed of three main modules, namely, packet-based physical (PHY) layer, spectrum sensing and multiple-access channel-sharing modules. The proposed framework is implemented using USRP Hardware Driver (UHD) software Application Programming Interface (API) [24] and runs on commercially available off-the-shelf (COTS) hardware devices such as the Universal Software Radio Peripheral (USRP) [25], which is a well-known platform for SDR development.

This paper is organized as follows. In section II, related works are compared with and distinguished from our work. Section III describes the proposed spectrum sharing framework for intelligent next generation wireless networks. Section IV presents in detail a highly flexible slot-based PHY that can be used in collaborative intelligent spectrum sharing research. Section V describes the RF monitor module and the spectrum

sensing algorithm used by this module to assess the medium state. Section VI introduces a totally configurable software based LBT module. Section VII presents some use cases with suggestions on how the proposed framework could be employed in intelligent next generation wireless networks. In section VIII, we present and discuss the results of several experiments performed with the proposed framework. Finally, section IX presents our conclusions and indicates directions for future work.

II. Related Work

Three of the most well-known open source LTE frameworks are Eurecom's OpenAirInterface (OAI) [26], openLTE [27] and Software Radio Systems' srsLTE [28]. OAI is compliant with LTE release 8.6 and implements only a subset of release 10. Additionally, it only supports 5, 10, and 20 MHz bandwidth and the code structure is complex and difficult to customize. OpenLTE's source code is well organized and can be customized to some extent, however, it lacks detailed documentation, e.g., there is no information on compliance with any 3GPP release and it has a very silent mailing list. Furthermore, it is still incomplete and with several features unstable or under development. On the other hand, srsLTE's source code is well organized with a modular structure, has good documentation, a very active mailing list and can be easily customized. However, it is only compliant with LTE Release 8 and implements a few features of Release 9. These open source frameworks can only be configured through configuration files (i.e., static configuration) and none of them offers any mechanism or feature for spectrum sharing.

The Amarisoft LTE-100 platform is a commercial and closed source SDR-based LTE network suite. This solution is compliant with 3GPP LTE Release 14 [29], however, as far as we are concerned, it does not support any of the features necessary for the operation in unlicensed bands, which are the base for spectrum sharing approaches. This platform can not be configured in real-time, only allowing file based configuration. The cost of the Amarisoft LTE-100 software suite ranges from 4500 to 8000 € depending on licensing type (fixed or floating) and number of channels. Moreover, as it is a closed-source solution, it can not be modified.

On the other hand there is the National Instruments' (NI) LabVIEW Communications LTE-Advanced Application Framework [30]. This proprietary framework implements a subset of the 3GPP LTE Release 10 and provides support for the FlexRIO PXIe-7975/7976R and USRP RIO devices. The LTE framework is easy to be modified, mainly due to LabView's graphical programming language, allows real-time prototyping and is extensively validated but has no built in coexistence feature. In [31], NI customized the LTE framework in order to implement some LTE-U and LTE-LAA features like discontinuous transmission and LBT. However, the customized framework can not be bought separately from the whole LabVIEW 802.11 and LTE-Advanced Application Frameworks, once it is sold as a Real-time LTE/Wi-Fi Coexistence Testbed. Additionally, the customized LTE framework can only be configured through a graphical user interface (GUI) and only allows threshold and Contention Window (CW) size parameters to be configured in real-time through the GUI. Moreover, this is a quite expensive solution, costing more than $66000.

A framework, named CONTACT, to explore emerging coexistence techniques among multiple Radio Access Technologies (RAT) in both wireless communication and computer networking is presented in [32]. The proposed framework is divided into three layers: radio access, network and control layers. However, the framework only implements a simple preemptive sharing scheme at the radio access layer, i.e., it implements Carrier-Sensing Adaptive Transmission (CSAT) to sense channel usage and adjust the on and off LTE cycling based on Wi-Fi usage [33]. Such schemes do not take collaborative and intelligent spectrum sharing into account and can not be deployed world-wide as some countries require the use of contention based access mechanisms [33]. The framework only allows real-time configuration of the ON/OFF duty cycle, however, the authors do not mention by which means (e.g., through pre-defined control messages over network) it is carried out. Additionally, the proposed framework is not publicly available either as open or closed source.

To the best of the authors' knowledge there is no open source framework that offers researchers and practitioners the flexibility and the necessary modules (i.e., LBT and RF monitor) to devise, implement and experimentally test novel spectrum sharing schemes. Additionally, none of the above mentioned solutions allows users to easily plug-in other modules, receive information and change parameters in real-time through pre-defined messages over the network. Table I summarizes the comparison of characteristics presented by each one of the related solutions.

Next, we list some related simulation works that can make use of the proposed framework to also validate the ideas through experimental validation.

In [34] the authors propose the use of particle swarm optimization to learn the behavior of spectrum usage, helping to allocate spectrum dynamically. They also introduce a intelligent and optimal relay selection algorithm for effective selection of relay nodes, which enhances amplify and forward relay selection algorithm using intelligent agents.

A spectrum allocation solution using multi-agent system cooperation that enables secondary users to utilize the amount of available spectrum, dynamically and cooperatively is proposed in [35]. The agents are deployed on primary and secondary users that cooperate to achieve a better spectrum usage.

A Q-Learning based dynamic duty cycle selection mechanism is proposed in [36] for the configuration of LTE transmission gaps, so that a fair coexistence, i.e., spectrum sharing, between LTE and Wi-Fi networks is guaranteed. Simulation results show that the proposed Q-Learning based approach improves the overall system capacity performance by 19 % and Wi-Fi capacity performance by 77% when compared to a scenario with fixed duty cycles where highest aggregate capacity is achieved. The results show that the approach

Preprints (www.preprints.org) | NOT PEER-REVIEWED | Posted: 1 October 2018 doi:10.20944/preprints201810.0017.v1

TABLE I
COMPARISON OF THE RELATED FRAMEWORK SOLUTIONS.

Framework	Open Source	Real-time configurability through control messages	RF Monitor	LBT	Discontinuous Tx	Cost
OAI [26]	Yes	No	No	No	No	-
openLTE [27]	Yes	No	No	No	No	-
srsLTE [28]	Yes	No	No	No	No	-
CONTACT [32]	No	Not informed	No	No	Yes	-
Amarisoft [29]	No	No	No	No	No	4500 to 8000 €
NI's LTE Framework [30]	No	No	No	No	No	> $66000

enables effective coexistence of LTE and Wi-Fi systems in the unlicensed spectrum bands.

In [37] the authors demonstrate that a Neural Network (NN) can accurately predict slots in a Multiple Frequencies Time Division Multiple Access (MF-TDMA) network. Through spectrum observation, the proposed Neural Network models are able to do online learning and predict the behavior of spectrum usage a second in advance. Results show that the proposed approach reduces the number of collisions by half when nodes follow a Poisson traffic distribution and a reduction by a factor of 15 when more periodic traffic patterns are used.

In [70] the authors propose a NN based approach that adapts LBT's CW size based on the predicted number of Negative Acknowledgments (NACKs) for all subframes in a Channel Occupancy Time (COT) of LTE-LAA. The correct configuration of the CW size is of utmost importance to avoid collisions or to resolve contention among colliding radios. The proposed approach learns from previous experiences how many NACKs per subframe of a COT were received under certain channel conditions. After the learning phase, it is able to predict the number of NACKs for all subframes in a COT without having to wait (at least 4 ms) for delayed HARQ feedbacks. The CW size is exponentially increased upon the reception of a NACK for each subframe of a COT. Results show that the proposed approach provides better trade-off between fairness to Wi-Fi and LTE-LAA in terms of throughput and latency when compared to state-of-the-art approaches.

All the above mentioned works propose novel ideas to improve the spectrum utilization, however, all the results are simulation based. These ideas need to be evaluated to check their limits and capabilities of achieving improved spectrum utilization with real-world equipment. Therefore, the aim of our work is to fill this gap by providing a framework that can be used to implement these ideas, assess and validate them trough experimental validation.

III. PROPOSED FRAMEWORK

In this section the proposed framework is described in details. The high level architecture of the proposed framework is shown in Figure 2.It is comprised of three main modules: (i) slot-based PHY layer (for discontinuous data transmission and reception), (ii) RF Monitor (for spectrum sensing purposes) and (iii) Listen Before Talking (LBT) (for Radio Access Technology (RAT) coexistence). All the main modules are connected to the ZeroMQ (Data/Control) module, which interconnects the framework with upper layers through the ZeroMQ bus [39]. This module manages the exchange of control and statistics messages between the framework and upper layers. The framework is used in conjunction with Ettus USRP X family of SDR devices including NI's RIO platforms [40, 41] and communicates with it through the UHD driver and its APIs [25].

USRP devices are hardware platforms developed for software defined radio (SDR), and are commonly used by research labs, universities, and hobbyists. USRP devices are controlled through the UHD driver. The driver provides an Application Programming Interface (API) that enables controlling and accessing all features provided by USRP devices, while abstracting the low level implementation details of the hardware. The most important operations provided by the UHD driver fall into two classes, namely, control and streaming. Control operations are used to set frequency, sample rate, gain, etc. of the radios. Streaming operations are carried out through streamer objects, which allow applications running on the host to connect to Tx and Rx sample streamers offered by the USRP device. These samples come from the radios available in the devices. An Rx streamer object allows applications to

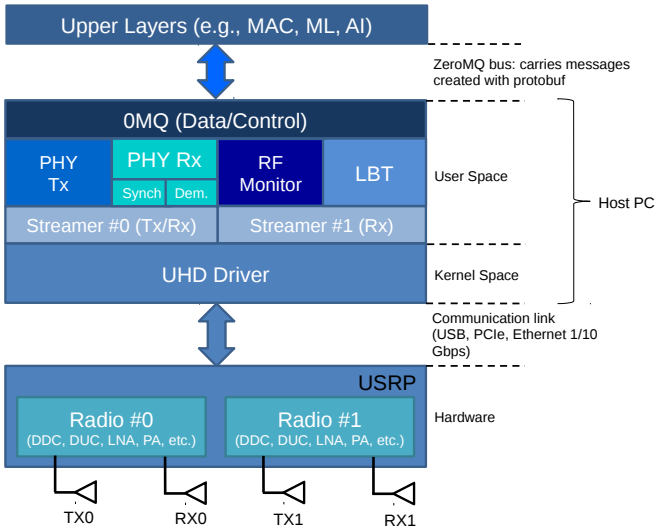

Fig. 2. Proposed Framework Architecture.

Preprints (www.preprints.org) | NOT PEER-REVIEWED | Posted: 1 October 2018 doi:10.20944/preprints201810.0017.v1

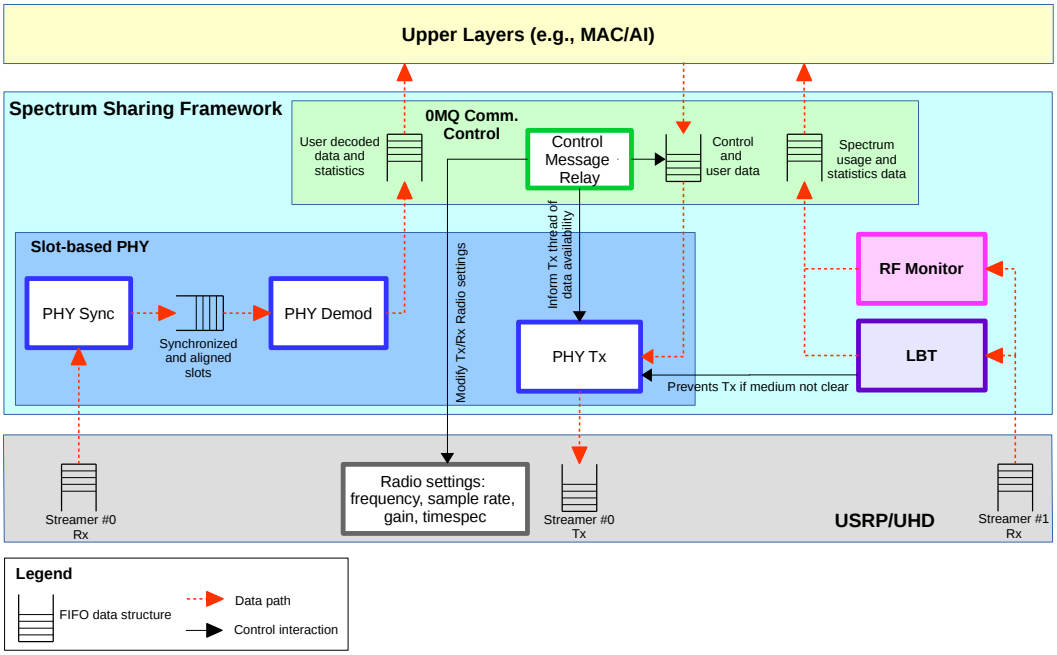

Fig. 3. Threading architecture of the proposed spectrum sharing framework.

receive samples from the device and a Tx streamer object allows applications to transmit samples to the device [25].

The slot-based PHY exclusively uses Streamer #0, both for Tx and Rx sample streams, and is fed by Radio #0. The RF Monitor and LBT modules share Streamer #1 (both of them only use the Rx sample stream), which is fed by Radio #1. Streamers #0 and #1 can be configured independently, i.e., different TX/RX frequencies, gains and samples rates can be set for each of them independently. For performance and priority management reasons, each of modules (ZeroMQ Data/Control processing, PHY Tx, PHY Rx Synchronization, PHY Rx Data Demodulation, RF Monitor and LBT) runs on an exclusive thread. The reason why PHY and the sensing modules (i.e., RF Monitor and LBT) use different and independent Streamers is due to the fact that we want to decouple their operations. The RF Monitor and LBT modules should use an exclusive streamer (i.e., Streamer #1) so that they can independently (from PHY RF parameters) and uninterruptedly (i.e., it is not desired to time-share a Streamer between PHY and the sensing modules) assess any configurable spectrum bandwidth at any desired center frequency and Rx gain. With this approach, both PHY and the sensing modules will always be receiving at their independently configured center frequencies, bandwidths and Rx gains without being affected by or affecting each other's operation.

Communication with the proposed framework is entirely realized through a well-defined interface (i.e., control and statistics messages) designed with Google's Protocol Buffers (protobuf) [42] for data serialization coupled with the ZeroMQ messaging library [39] for distributed exchange of control messages and data. Implementing the ZeroMQ push-pull pattern allows local or remote upper layers' real-time configuration of several parameters and reading of several pieces of information/statistics provided by the framework. Based on the ZeroMQ logic, all modules are able to exchange control and data messages following an non-blocking communication paradigm. Additionally, by adopting protobuf and ZeroMQ, the proposed framework offers other modules/layers the flexibility to use any kind of programming language implementation, making it easier to integrate multiple independent modules into a single working system. The flexible communication interface provided by the framework makes it ideal for deployment in testbeds and allows different upper layers to be plugged in, hence, an important enabler for intelligent spectrum sharing experimentation towards next generation of wireless networks.

Figure 3 illustrates the different layers composing the proposed spectrum sharing framework and the threads within each one of them. Red dashed arrows indicate data paths while black arrows indicate control/information interaction between threads.

Through the use of the proposed framework, a myriad of real-world experiments can be performed, ranging from research of new physical layer techniques (e.g., higher order modulation schemes, novel waveforms and numerologies, channel coders, etc.) to RAT coexistence in unlicensed and licensed shared spectrum bands (e.g., comparison of the fairness between different contention-based mechanisms such as Carrier Sense Adaptive Transmission (CSAT) and LBT, impact of different parameters such as COT, idle time, Tx power, PHY bandwidth, spectrum overlap, Modulation Code Scheme (MCS) on the performance of Wi-Fi and LTE networks, etc.) to collaborative and intelligent radio networks (i.e., networks where AI and ML components act as the brain of the system

Preprints (www.preprints.org) | NOT PEER-REVIEWED | Posted: 1 October 2018 doi:10.20944/preprints201810.0017.v1

and control various aspects of medium access and PHY layers to ensure adaptability, while also running some sort of collaboration protocol [43, 44]).

In the next sections, we describe each one of the main modules present in the proposed framework.

IV. Slot-based Physical Layer

In spectrum sharing scenarios, several networks might share the medium at the same time and therefore continuous access to it may not be possible all the time. With discontinuous transmissions, it is possible to have a better use of the available spectrum band and to coordinate its usage with other networks in an opportunistic/intelligent/collaborative way. Continuous access is the preferred approach for systems operating in exclusive licensed bands where there is no need for sharing, and is not really suited to fair medium sharing between co-located networks. Moreover, in unlicensed spectrum, some regulatory authorities do not allow continuous transmissions and limit the maximum duration of a transmission burst [45].

A PHY layer supporting a discontinuous transmission feature would be a great value for spectrum sharing research, as it could be used to leverage techniques devised to achieve fairer coexistence and higher spectral efficiency in scenarios where time-frequency resources are shared. Hence, as part of our framework for spectrum sharing research, we decided to develop a discontinuous transmission-based PHY, which transmits data bursts in small transport units called slots. A slot is the container through which data is exchanged in the network.

We have based the development of the proposed slot-based PHY on the LTE PHY standard, as it offers several advanced features including high spectrum efficiency, multiple bandwidths, high peak data rates, mobility, multi-user access, flexible time framing and time-frequency structure, link adaptation with adaptive modulation and coding schemes and multiple-input and multiple-output (MIMO) [46, 47]. Moreover, the next generation of wireless networks (i.e., 5G) will naturally evolve from LTE -based standards [46], i.e., they will be made available through improvements in LTE, LTE-Advanced and LTE-Advanced Pro technologies [48]. Consequently, building upon the LTE PHY standard makes it easier to further extend the slot-based PHY in compliance with 5G standards and further evolutions. The proposed slot-based PHY is built upon the srsLTE open source library [28], and therefore, absorbs and evolves on top of the existing LTE features.

In order to stay aligned with both LTE standards and 5G initiatives [47, 48], we decided to adopt an Orthogonal Frequency-Division Multiplexing (OFDM) based waveform. OFDM is a mature technology, which is vastly implemented in a great number of products due to its advantages such as robustness to severe multipath fading, low implementation complexity, easy integration with MIMO, simple channel estimation, etc. [47]. Additionally, OFDM allows for enhancements such as waveform windowing/filtering, which can effectively minimize out-of-band spurious emissions [49]. It is also worth mentioning, that compared to other popular OFDM-based technologies like Wi-Fi [50] and Digital Video Broadcasting-Terrestrial (DVB-T) [51], LTE was devised since its inception for multi-user communications by assigning subsets of 12 subcarriers (also known as a physical resource block (PRB) or only resource block (RB)) over multiple 1 ms long subframes to individual users. This flavor of multiple access is known as Orthogonal Frequency-Division Multiple Access (OFDMA) and gives LTE a very flexible way of allocating time/frequency resources to multiple concurrent users.

As mentioned earlier, the proposed slot-based PHY module is split into three submodules, namely, PHY Tx, PHY Rx Synchronization and PHY Rx Demodulation where each one of them runs on an exclusive, standalone thread. The reason for having a multi-threaded PHY implementation is that it allows independent critical and/or time-consuming tasks to be executed simultaneously (i.e., concurrently). Computing performance and efficiency is improved by taking advantage of concurrency. Allied with multi-core enabled Central Processing Units (CPUs), the multi-threaded PHY naturally supports full-duplex communications mode, i.e., one PHY can simultaneously transmit and receive at different frequencies, which consequently results in a higher throughput. PHY Tx thread is responsible for modulation and transmission of data (i.e., user and control data). PHY Rx Synchronization thread is responsible for the Primary and Secondary Synchronization Signal (PSS/SSS) detection, time synchronization, Carrier Frequency Offset (CFO) correction and slot alignment tasks. PHY Rx Demodulation thread takes care of user and control data demodulation, i.e, OFDM demodulation, PDCCH search and PDSCH decoding. The slot-based PHY receives data and control messages from the ZeroMQ Data/Control module.

Regarding numerology, the proposed PHY supports LTE numerology with the same subcarrier spacing (15 kHz) and the cyclic prefix (CP) lengths (normal and extended CPs). However, the proposed PHY also supports the configuration of different (larger and smaller) subcarrier spacings and CP lengths by adopting different sampling rates. Larger subcarrier spacing is used to mitigate inter-carrier interference (ICI) at high frequency bands and smaller spacing allows for extended coverage (due to increased Power Spectral Density (PSD)) and high delay spread scenarios (due to longer CP) at low frequency bands [47, 48].

Different CP lengths are used to accommodate different levels of inter-symbol interference (ISI) at different frequencies, coverage and mobility [48]. All LTE predefined bandwidths (1.4, 3, 5, 10, 15 and 20 MHz) are supported. PHY channel bandwidth (BW) can be changed through command line at start up, or in real-time, through one of the control messages, which are introduced later in this section.

Differently from the LTE PHY downlink, which is continuously transmitting signals, the proposed slot-based PHY employs discontinuous (i.e., bursty) transmission of slots. A slot is the basic transmission unit of the proposed PHY and each one is 1 ms long. Depending on its type, a slot might carry synchronization signals, reference signals, broadcast, control and user data.

Preprints (www.preprints.org) | NOT PEER-REVIEWED | Posted: 1 October 2018 doi:10.20944/preprints201810.0017.v1

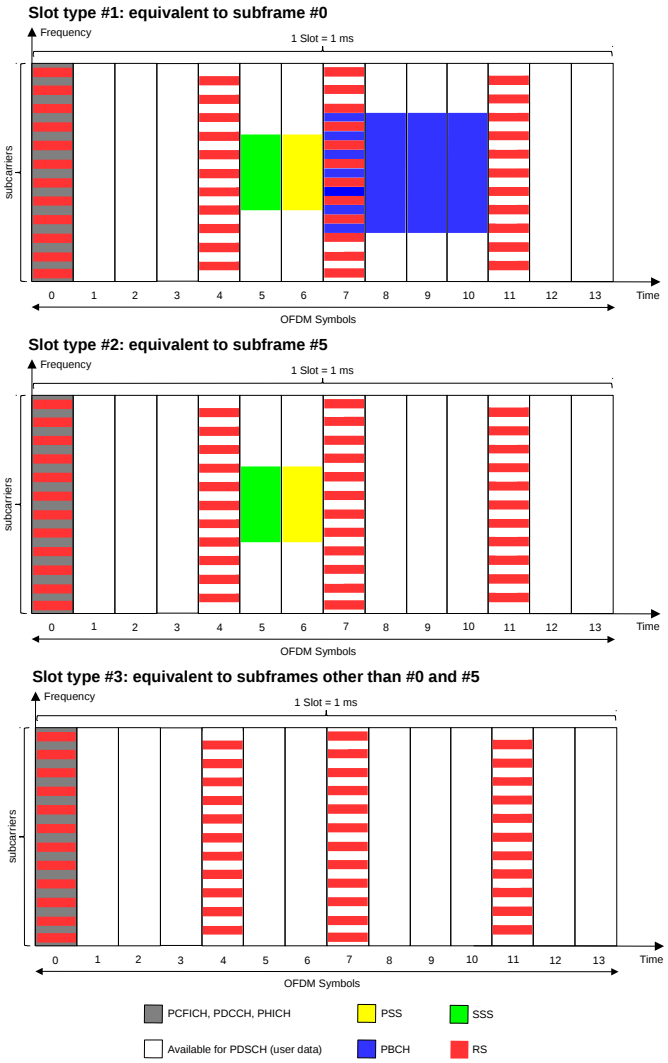

Fig. 4. Proposed slot types for normal CP length.

Three different types of slots, following the same definition as the LTE subframes, are proposed [46, 47]. All the slot types for the normal CP length are depicted in Figure 4. The first type, which is equivalent to subframe #0 in the LTE standard, carries synchronization signals (PSS/SSS), reference signals, broadcast, user and control data. The second type is equivalent to LTE's subframe #5 and carries synchronization signals (PSS/SSS), reference signals, user and control data. The third type, which is equivalent to LTE's subframes other than 0 and 5 (i.e., 1 to 4 or 6 to 9), only carries reference signals, user and control data. It is important to notice that the RBs intended to carry user data can be split into different sections and allocated to different concurrent users. All slots types carry user data, signals for channel estimation/equalization, and control data, which holds information on how to decode each one of the possible user data sections. The first two slot types are used for transmission detection, as they carry synchronization signals. The first slot one is used whenever there is a need to transmit broadcast information. As it does not carry synchronization signals, the third type can only be used when transmitted after one of the other two types. Similarly to an LTE subframe, each slot can have 14 or 12 OFDM symbols depending on the configured CP length, i.e., normal or extended CP [46]. Moreover, each one of the three slot types is self-decodable as they always carry control data. The control data part of the slot is used at the PHY receiver side to automatically detect the number of allocated RBs and the MCS used to transmit data of a specific user. By following this approach, upper layers do not need to specify the number of RBs and MCS before every slot reception. Upon correct user data reception, PHY informs the upper layers the number of received bytes and the corresponding MCS.

The proposed PHY allows bursty transmissions with variable COT, i.e., the number of slots to be transmitted in a row without any gap (i.e., idle time) between them is variable. The number of slots in a COT, i.e., frame, is derived based on MCS, number of Resource Blocks (RB) and data length (i.e., number of bits to be transmitted) parameters sent by upper layers in the control messages. The minimum COT is equal to 1 ms and is equivalent to a slot. Variable COT enables the support of different traffic loads. Every slot can carry a pre-defined number of bits, which is based on the MCS and number of RBs used for a transmission [47].

The proposed PHY can operate with two different data transmission modes. The first mode can be used to establish communications with multiple nodes in ad-hoc or mesh networks, depending on routing capabilities implemented in the upper layers connected to the slot-based PHY (i.e., routing at layer 3 of the OSI model). This mode is a simplification of the LTE channel's structure and only uses the Physical Downlink Shared Channel (PDSCH) for user data transmissions in both directions, i.e., downlink and uplink, in order to take advantage of both multi-user communications and high performance Forward Error Correction (FEC) provided by turbo codes [47]. Additionally, this mode also uses Physical Control Format Indicator Channel (PCFICH) and Physical Downlink Control Channel (PDCCH) for control purposes and Cell-specific Reference Signals (CRS) for channel estimation and equalization. The second mode operates exactly with the same channel's structure as adopted in the LTE standard, i.e., it has all downlink and uplink physical layer channels as defined in the standard. This mode can be used to establish communications in a cellular mobile network. In both modes, OFDMA can be used to communicate with multiple users at the same time.

Regarding frame structures, we propose two different types, as depicted in Figure 5. In the first one, PSS and SSS sequences are added to all slots in a COT, allowing for better time-frequency tracking at the receiver side. This frame structure allows the receiver to easily perform slot synchronization every 1 ms without the necessity of complex tracking algorithms. However, as PSS and SSS signals are added to all slots, it is not possible to reach MCS values higher than 25 as those signals occupy several subcarriers that could be used for user data transmission. Another downside is that

Preprints (www.preprints.org) | NOT PEER-REVIEWED | Posted: 1 October 2018 doi:10.20944/preprints201810.0017.v1

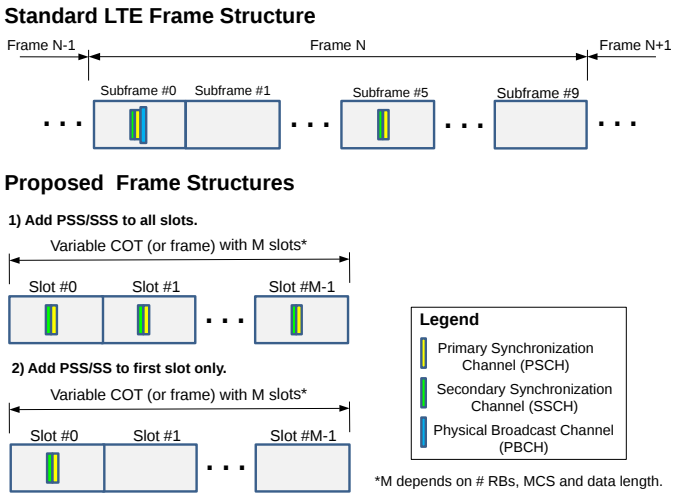

Fig. 5. Standard LTE versus Proposed Frame Structures.

PSS and SSS detection is time-consuming and consequently, decreases the maximum achievable throughput as the period of time required to detect and decode slots increases. In the second proposed frame structure, PSS and SSS signals are added only to the first slot of a COT. This structure increases the number of subcarriers useful for user data transmission (making it possible to reach the highest MCS value, i.e., 28 [52]) and decreases the time to receive and decode slots, consequently improving the throughput. However, this frame structure requires a more complex tracking/synchronization algorithm and the necessity to add information about the number of slots in a COT to the first slot, which means, if the first slot is lost none of the subsequent slots can be decoded.

The first proposed frame structure is more robust to time and frequency fluctuations and should be used in cases where transmitter and receiver nodes are moving as it provides better synchronization and less slot losses. On the other hand, the second frame structure should be used for static or quasi-static nodes. The proposed PHY allows switching between the two frame structures either through command line at initialization or during run-time in order to adapt itself to different radio link conditions.

The Payload Data Unit (PDU) adopted by the proposed PHY is a Transport Block (TB), which is a concept reused from LTE PHY layer. Therefore, a TB is the payload coming from upper layers and given to PHY to be transmitted over the air through the PDSCH. A TB is defined in the LTE standard and varies according to some parameters [53]. According to the LTE standard, 1 TB consists of a number of bits that can be accommodated within a 1 ms long subframe given the selected number of RBs and MCS [53]. Therefore, given the number of allocated RBs and the desired MCS, upper layers can find the number of bits that can be handled by an 1 ms long slot.

The communication between upper layers, e.g., Medium Access Control (MAC), and the proposed PHY layer is carried out through the exchange of four messages. The first two, namely, Tx and Rx Control messages, are used to manage

TABLE II
SLOT-BASED PHY REAL-TIME CONFIGURABLE PARAMETERS AND STATISTICS.

Message	Parameter	Type	Unit	Range
Tx control	Number of RBs	uint32	-	1-100
	MCS	uint8	-	0-28
	Tx gain	uint32	dB	depends on HW [1]
	Tx channel	uint32	-	≥ 0
	Tx PHY BW	uint8	MHz	0-6 [2]
	Transmission timestamp	uint64	s	≥ 0
	Frame structure type	uint8	-	0/1 [3]
	Data length	uint32	-	> 0
	User data	uchar[]	-	uchar range
Rx control	Rx channel	uint32	-	≥ 0
	Rx gain	uint32	dB	depends on HW [1]
	Rx PHY BW	uint8	MHz	0-6 [2]
Rx statistics	CQI	uint8	-	0-15
	RSSI	float	dBW	float range
	Noise	float	dBW	float range
	Decoded MCS	uint8	-	0-28
	Slot error counter	uint32	-	≥ 0
	Decoding time	uint32	ms	≥ 0
	Data length	uint32	-	≥ 0
	Received data	uchar[]	-	uchar range
Tx statistics	Coding time	uint32	ms	≥ 0
	Number of transmitted slots	uint32	-	≥ 0

slot transmission and reception respectively. The parameters carried by these two messages can be configured and sent to PHY by upper layers before the transmission of every slot, hence allowing runtime configuration. The other two messages, namely, Tx and Rx statistics messages, are used to give real-time feedback from PHY to upper layers, providing vital information necessary for such layers to take actions.

Tx control messages carry the user data (i.e., TB) to be transmitted and Tx parameters related to that transmission such as number of RBs, MCS, data length, Tx gain, Tx channel, Tx PHY BW, transmission timestamp and frame structure type. The transmission timestamp parameter enables time-scheduled transmissions, which allows the implementation of Time Division Duplexing (TDD) or Time Division Multiple Access (TDMA) technologies with the proposed PHY layer. **Rx control** messages are used to configure Rx channel, Rx gain and Rx PHY BW.

The other two messages, namely, Rx and Tx statistics, are used to inform upper layers of PHY Rx and Tx processing results respectively. **Rx statistics** messages carry the received data and reception statistics related to the received data such as Channel Quality Indicator (CQI), Received Signal Strength Indication (RSSI), decoded MCS, slot error counter, decoding time, etc. **Tx statistics** messages inform upper layers of transmission statistics like coding time, total number of transmitted slots. Table II summarizes all the real-time configurable parameters and statistics offered by the slot-based PHY.

Figure 6 depicts the GUI provided by the slot-based PHY, which can be used for debugging or demonstration purposes. The GUI plots the constellation diagram of equalized and decoded PDSCH and PDCCH symbols (upper and lower left respectively), the equalized channel response (upper right) and the correlation peak of the PSS (lower right).

Preprints (www.preprints.org) | NOT PEER-REVIEWED | Posted: 1 October 2018 doi:10.20944/preprints201810.0017.v1

A. Filtered-OFDM

As it is well-known, OFMD-based waveforms are not suited for spectral coexistence due to its poor spectral localization [54]. This problem is caused by the rectangular pulse-shape used in OFDM, which leads to a sync-pulse property in the frequency domain with a very low second lobe attenuation of -13 dB [55].

One of the simplest but still very efficient approaches used to guarantee better spectral localization, i.e., lower out-of-band (OOB) emissions, and maintain the complex-domain orthogonality of the OFDM symbols is to apply some sort of filtering to the time domain OFDM symbols, giving rise to a new waveform known as Filtered-OFDM (f-OFDM) [56].

Appropriate filtering of the OFDM signal must satisfy the following criteria: (i) have a flat passband over the subcarriers in the sub-band; (ii) have a sharp transition band to minimize guard-bands; (iii) have sufficient stop-band attenuation. A Finite Impulse Response (FIR) filter with a rectangular frequency response, i.e., a sinc-pulse impulse response, meets these criteria. To make this causal, the low-pass filter is realized using a window, which, effectively truncates the impulse response and offers smooth transitions to zero on both end [57].

Therefore, a FIR filter meeting the necessary requirements is added to the Tx processing flow, just after the OFDM modulation. The filter is applied just before the OFDM symbols are sent to the hardware, e.g., USRP. An efficient FIR is implemented on software making use of Single Instruction Multiple Data (SIMD) instructions present on most of the general purpose microprocessors, i.e., central processing units

[1]Depends on the USRP daughter board installed [25].

[2]The numbers correspond LTE bandwidths: 1.4, 3, 5, 10, 15 and 20 MHz respectively.

[3]The numbers correspond to frame structure types where PSS/SSS signals are added to all slots in a burst and PSS/SSS signals are only added to the first slot in a burst respectively.

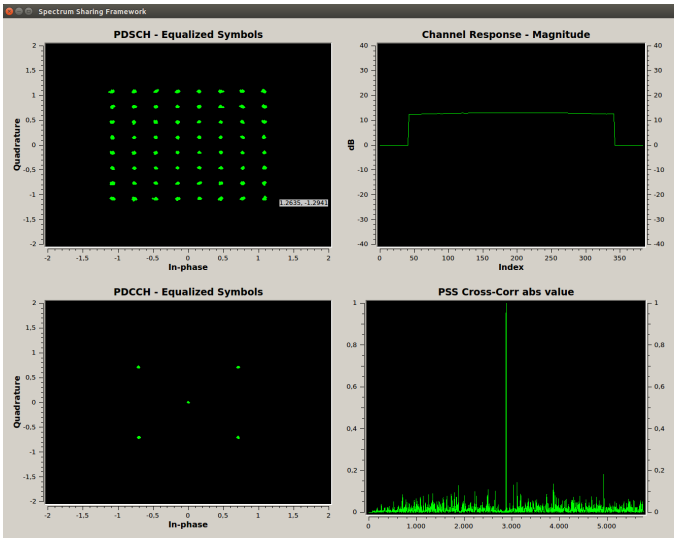

Fig. 6. Slot-based PHY graphical user interface.

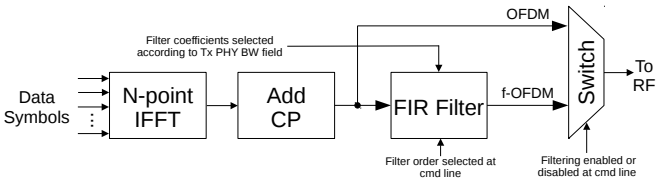

Fig. 7. Filtered-OFDM enabled transmitter.

(CPUs), available today to exploit the data-level parallelism present in the filtering processing. The filter's coefficients applied to the modulated OFDM signal are automatically selected according to the configured Tx PHY BW (i.e., the coefficients are selected in real-time based on the Tx PHY BW field in the Tx control message) as it needs to have its cut-off frequency changed to exactly filter the desired signal's bandwidth. Figure 7 shows the f-OFDM enabled transmitter scheme, which can have the FIR filtering processing enabled or disabled and the filter order selected at command line during start up of the framework.

B. Advantages of the proposed slot-based PHY

In this section we describe the main advantages offered by the proposed slot-based PHY. The first advantage is that there is no need to align the start of transmissions to subframe boundaries. This is in contrast to LTE-LAA, where reservation signals are transmitted in order to prevent other RATs (e.g., Wi-Fi) from initiating a transmission until the next subframe boundary. The transmission of reservation signals clearly reduces the utilization efficiency of the available radio resources. As the proposed PHY adopts bursty transmissions, all the information required for synchronization and demodulation is self-contained in every slot. This allows for the development of standalone solutions that do not need to use reservation signals and to be subframe-aligned to an anchor on licensed spectrum.

A second advantage of the proposed PHY is that the filtering applied to the OFDM symbols makes the filtered-OFDM PHY more spectral efficient as the OOB emissions are reduced. To be more specific, in LTE, 10% of the allocated bandwidth is reserved as guard band, which allows the waveform signal to attenuate and therefore, meet the spectrum mask requirements [58]. Undoubtedly, this is a considerable waste of frequency resources, which are becoming more precious. Additionally, OOB emissions interfere with other nearby allocated systems, decreasing the quality of the received signal, which impacts on the throughput experienced by that system. The reduced OOB emissions make the proposed PHY ideal for coexistence with other RATs (e.g., incumbent systems, spectrum sharing RATs, etc.), allowing it to operate closer to other systems in frequency domain and consequently, reducing spectrum wastage while increasing the spectral efficiency as shown in Figure 8.

Another advantage, offered by the proposed framework, is the possibility to configure in real-time all PHY (and also RF Monitor and LBT modules) parameters through pre-defined control messages, which can also be easily modified (thanks to

Preprints (www.preprints.org) | NOT PEER-REVIEWED | Posted: 1 October 2018 doi:10.20944/preprints201810.0017.v1

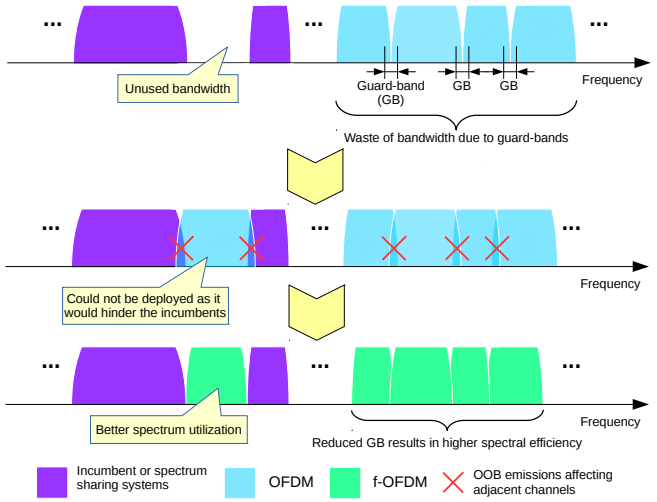

Fig. 8. Closer coexistence to other RATs due to reduced OOB emissions.

the use of Google's protobuf interface description language) to accommodate new parameters. By plugging in a new module to the system, it is possible to experiment with the PHY parameters in a programmatically way, so that new algorithms can be developed and tested.

V. RF Monitor

As mentioned earlier, this module runs on an exclusive thread and utilizes Radio # 1 of the USRP to act as a spectrum sensing monitor. It monitors and reports on a defined range of spectrum band and can be configured to report either the detected power per subband or subband occupancy (statistical hypothesis testing [59]), i.e., if a subband is free or already being occupied by another transmitter. Figure 9 depicts the architecture of the RF Monitor module.

Subband power reporting is obtained by applying a N-point FFT to the received IQ samples, summing the squared modulus of every consecutive B FFT bins (where B must be a power of two) to form M groups of power samples, i.e., subbands and then, applying the base-10 logarithm in relation to a reference power of 1 Watt to each one of the subbands, resulting in measurements given in dBW. A M-long float array holds the subband power information.

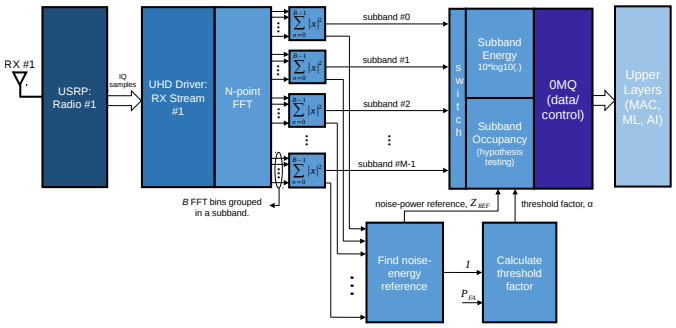

Fig. 9. RF Monitor architecture.

In order to report subband occupancy, the module implements a spectrum-sensing algorithm based on a Cell-Average Constant False Alarm Rate (CA-CFAR) strategy [59, 60]. The proposed algorithm is composed of three stages: (i) identification of a set of power samples, I, that can be considered as containing only the presence of noise in order to calculate a noise-power reference value, Z_{REF}; (ii) the number of power sample values considered for the calculation of the noise-power reference value, and the desired probability of false alarm, P_{FA}, are used in the second stage to calculate the detection factor, α; (iii) the third stage employs both, the threshold factor and the noise power reference value to test the occupancy of each one of the subbands.

The power samples used in the first stage are also obtained after applying an N-point FFT to the received IQ samples and summing the squared modulus of every B FFT bins into subbands. The procedure used to find the noise-power reference value, Z_{REF}, in the first stage involves ordering the subbands in ascending order of power. The detection threshold is found by multiplying Z_{REF} by the threshold factor, α. In the end, there are M subbands which will be tested against the detection threshold, in order to declare whether the subband is occupied or free. If the subband power is greater than the detection threshold, then the subband is declared occupied (true), otherwise it is declared free (false). After testing all subbands, an M-long boolean array holds the occupancy information of the monitored spectrum band. In the current implementation, the probability of false alarm, P_{FA} is set to 10^{-4}. Further information on this algorithm can be found in [59] and the references therein.

The module allows configuration of the following parameters for both types of reporting (power or occupancy): monitored bandwidth (through the change of the sampling rate), center frequency, number of FFT bins M, which changes the frequency resolution, Rx gain, considered as a subband (i.e., number of bins considered for the subband power calculation) and periodicity of the report of statistics. These parameters can be configured in real-time by upper layers through the **RF Monitor control** message. The sensing reporting type, i.e., power or occupancy, is configured during initialization of the framework. The following information is sent to upper layers through an **RF Monitor statistics** message: timestamp of the moment the IQ samples were received by the USRP and power or occupancy array depending on the configured reporting type. Table III summarizes all the real-time configurable parameters and statistics offered by the RF monitor module.

The RF monitor module is of great importance to spectrum sharing mechanisms as it offers a local insight of the spectrum band usage. It allows upper layers to access spectrum sensing measurements, which can be used to train ML and AI modules to better understand the environment, optimize the spectrum usage/sharing and cooperatively work with other networks without any previous knowledge on the other network's operation and implementation, i.e., without any co-design [61]. For instance, this module allows the implementation of adaptive carrier selection algorithms such as CSAT [62] and can also

Preprints (www.preprints.org) | NOT PEER-REVIEWED | Posted: 1 October 2018 doi:10.20944/preprints201810.0017.v1

TABLE III

RF MONITOR REAL-TIME CONFIGURABLE PARAMETERS AND STATISTICS.

Message	Parameter	Type	Unit	Range
RF Monitor control	Monitored bandwidth	float	Hz	depends on HW [1]
	Center frequency	float	Hz	depends on HW [1]
	Rx gain	uint32	dB	depends on HW [1]
	Number of FFT bins	uint32	-	16-16384
	Report periodicity	uint32	μs	≥ 150
RF Monitor statistics	IQ samples timestamp	uint64	s	≥ 0
	Power/Occupancy array	float[]/bool[]	-	float range or True/False

be used to train ML or AI modules to perform MF-TDMA slot allocation [37].

VI. LISTEN BEFORE TALK

As the other modules in the proposed framework, the software-based Listen Before Talk (SW-based LBT) module also runs on an exclusive thread. The module implements a contention-based mechanism for medium access based on 3GPP's LAA specifications [63, 64]. However, differently from 3GPP's LAA specifications, the proposed implementation allows the following configurations: minimum and maximum contention window (CW) sizes (with the option for the upper limit to be fixed or dynamically adjusted), variable frame period (with configurable maximum COT and clear periods, which allows longer than the standardized maximum frame period [63] and the adaptation to different traffic loads and channel usage [65]) and threshold. Figure 10 shows the proposed variable frame structure supported by the implemented LBT module. The frame period, which is composed of the COT and clear periods, can be dynamically configured to any value greater than 1 ms.

The rationale behind the decision to implement a SW-based LBT module is explained next. We start by presenting in Table IV round trip time (RTT) measurements for an x310 USRP device combined with different communication links. Notice that, each latency measurement is calculated as the average over 10 trials for each one of the following sampling rates: 5, 10 and 25 MHz. The measurements show that compared to the 1 ms long slot of the proposed PHY, it is feasible to use a SW-based LBT implementation as the RTT is of approximately 100 [us]. The SW-based implementation avoids the development an FPGA-based LBT module, which allows the framework to be used and ported to a wider range of SDR devices. Additionally, the SW-based implementation makes the LBT module easier to be customized by a wider range of users, as FPGA development is not so widespread and straightforward as software development.

Figure 11 depicts the Finite State Machine (FSM) of the proposed SW-based LBT module, which is explained as follows. Initially, a radio having data to transmit performs

TABLE IV

ROUND TRIP TIME BETWEEN UHD AND X310 USRP DEVICE [66].

Link Type	RTT [us]	Host PC configuration
PCIe	79	Intel i7-6700 3.4GHz, NI PCIe x4 card
10 Gbps ETH	106	Intel E5-2650 v4 2.2GH, Qlogic 57810 ETH
1 Gbps ETH	101	Intel i7-6700 3.4GHz, Intel i219-v ETH

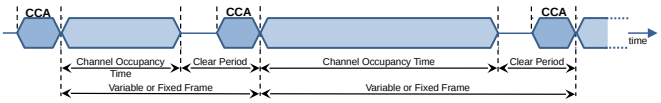

Fig. 10. SW-based LBT frame structure.

a Clear Channel Assessment (CCA) in order to determine if the medium is occupied or clear, i.e., the radio performs energy detection (ED) in given spectrum band during CCA observation time, if the measured energy level exceeds the CCA threshold then the medium is declared as occupied, otherwise, the medium is clear. If the radio finds the medium clear, it may transmit immediately and occupy the medium for the total time of COT.

In case the medium is occupied, the radio must execute a random backoff procedure, where a backoff counter is set to a random number, Q, drawn from a specified interval called the CW [67]. During the random backoff procedure, Q CCA checks are performed for the duration of a CCA observation time, where Q defines the total number of clear periods that need to be observed (i.e., counted) before the radio can transmit. The backoff counter is decremented every time the medium is observed to be clear. The radio may transmit when the counter reaches zero. The random backoff procedure was designed to cope with situations where more than one radio senses the medium as in clear state at the same time, and with this, decreasing the collision probability.

The CW size can be configured to be fixed or dynamic, with adjustable minimum and maximum values. In the fixed mode, Q is always drawn from the same interval, giving different radios the same probability of transmission opportunity in spite of collisions and traffic load. This approach is not fair when coexisting with RATs that adopt exponentially increasing CWs (e.g., Wi-Fi) when a collision happens. In the dynamic mode, a binary exponential backoff mechanism is used in the way that the CW size is increased exponentially based upon the occurrence of a collision (which can be based on feedback reports such as HARQ ACK/NACK or based on channel utilization sensing [68]) and reset to the minimum value when the transmission succeeds. The dynamic mode was devised to improve the overall channel utilization, reduce the collision probability and fairly coexist with other RATs like Wi-Fi.

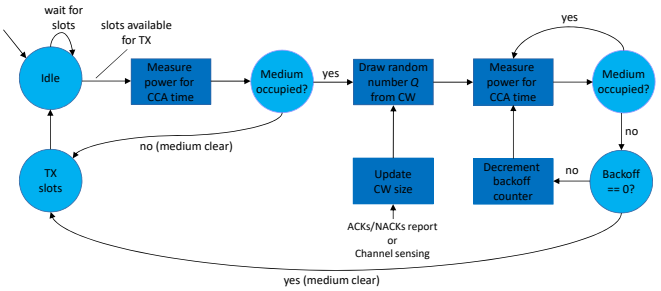

Fig. 11. Software-based LBT FSM.

Preprints (www.preprints.org) | NOT PEER-REVIEWED | Posted: 1 October 2018 doi:10.20944/preprints201810.0017.v1

TABLE V

LBT REAL-TIME CONFIGURABLE PARAMETERS AND STATISTICS.

Message	Parameter	Type	Unit	Range
LBT control	Sampling rate	float	Sps	depends on HW [1]
	Center frequency	float	Hz	depends on HW [1]
	CCA threshold	float	dBW	float range
	CCA observation time	uint32	μs	> 0
	CW type	uint8	-	0/1 (fixed/dynamic)
	Minimum CW value	uint32	-	≥ 0
	Maximum CW value	uint32	-	≥ 0
	Idle time	uint32	μs	≥ 0
LBT statistics	Channel clear ratio	float	-	0-100 %
	Channel clear avg. energy	float	dBW	float range
	Channel occupied ratio	float	-	0-100 %
	Channel occupied avg. energy	float	dBW	float range

The following parameters can be configured in real-time by upper layers through an **LBT control** message: sampling rate, center frequency, CCA threshold, CCA observation time, CW type (fixed or dynamic), CW minimum and maximum values and idle time. Additionally, the proposed LBT design keeps track of the following channels' occupancy statistics: channel clear/occupied ratios and clear/occupied average energies. These statistics are reported to upper layers through an **LBT statistics** message and can be used, for example, to find the optimum channel to be used, i.e., the least occupied channel. Table V summarizes all the real-time configurable parameters and statistics offered by the LBT module.

VII. USE CASES

In this section we describe three use cases for the proposed framework. The first one focuses on how the framework may facilitate slot selection in time and frequency domains in order to coexist with other technologies, based on intelligent prediction of the medium usage. The second use case shows how the framework can allow contention-based parameters at MAC level to be optimized when an intelligent upper layer is integrated for specific technologies. The third one shows how the framework can be used to devise and test flexible spectrum sharing paradigms.

A. Transmission Pattern Prediction

In the unlicensed 5 GHz spectrum band, RATs such as LTE-U, LTE-LAA and Wi-Fi use the same spectrum for communications, which often results in cross-technology interference, i.e., interference from spatially close concurrent transmissions that overlap in time and frequency, an event known as collision.

In order to mitigate cross-technology interference, in this use case, the proposed framework is used to implement an intelligent Multi-Frequency Time-Division Multiple Access (MF-TDMA) like network in a congested unlicensed spectrum. Here, the slot-based PHY and the RF Monitor modules are integrated with a MAC layer and a reasoning module featuring a Neural Network (NN) model.

The NN is trained to improve slot scheduling (i.e., time/frequency allocations) by predicting transmission patterns, and consequently avoiding traffic from other nodes regardless of the technologies they are using. By observing the spectrum, through statistics received from both the RF Monitor and PHY modules, the NN is able to do online learning and predict the behavior of other nodes, finding free slots some time in advance. Based on the slot usage predictions provided by the reasoning module, the MAC layer can select in advance the best channel and the necessary COT and MCS to deliver the traffic load while not causing interference (i.e., collisions) to other radios. Figure 12 shows how the integration of the proposed framework with a reasoning module can be used to implement an intelligent spectrum sharing scheme.

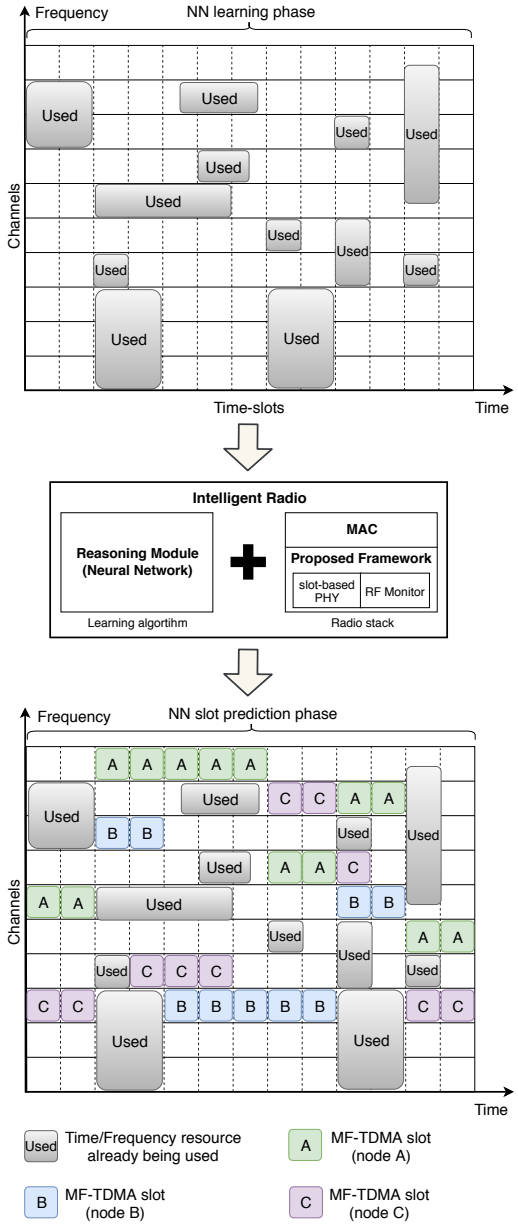

Fig. 12. Use case scenario: MF-TDMA free slot prediction.

B. Intelligent LTE-LAA and Wi-Fi Coexistence

LTE-LAA enables the deployment of LTE networks in the unlicensed 5 GHz spectrum band. However, when coexisting with LTE-LAA, the performance of Wi-Fi networks primarily

Preprints (www.preprints.org) | NOT PEER-REVIEWED | Posted: 1 October 2018 doi:10.20944/preprints201810.0017.v1

relies on how the LTE-LAA parameters are configured, especially parameters such as channel, COT, idle time and CW size that govern the transmission opportunities in LTE-LAA networks.

In order to provide fairer coexistence (i.e., provide fair opportunities for all technologies to access the medium), LTE-LAA parameters must be dynamically configured based on specific statistics like collision counters, different channel utilizations, i.e., the traffic load present in a channel, etc. In this use case, the proposed framework is used to implement an intelligent LTE-LAA base station (BS). Here, the slot-based PHY and the LBT modules are integrated with a Reinforcement Learning (RL) module, which can feature algorithms like Multi-Armed Bandit or Q-Learning, to maximize the overall capacity performance through an efficient coexistence.

The RL module learns how to estimate the activity of Wi-Fi users and consequently adjust the LTE-LAA parameters for several traffic conditions. The main goal is to determine a policy by which the LTE-LAA BS can intelligently choose the optimum channel, COT, idle time and CW size based on collision statistics and measurements taken during the sensing period. Figure 13 shows how the integration of the proposed framework with an RL module can be used achieve efficient RAT coexistence. In the figure, we see in the upper part the sensing period, where the RL module learns about the medium usage, i.e., how often and how long others networks access the channels. Based on what the module learned, we see in the lower part of the figure that the LTE-LAA node is able to select channels that can accommodate its traffic load needs.

C. Coordinated Spectrum Sharing Schemes

The adoption of spectrum sharing mechanisms is expected to bring critical benefits to the next generation of wireless networks. For example, spectrum sharing can unlock additional, currently underutilized, spectrum bandwidths, make it possible to introduce new deployment scenarios and improve spectrum utilization [69, 70].

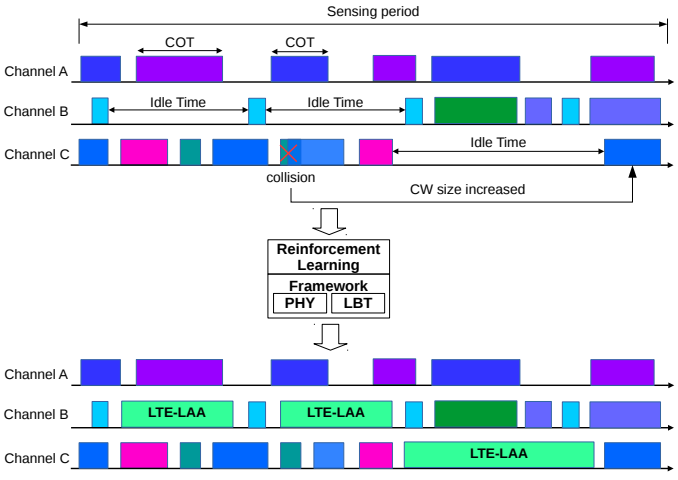

Fig. 13. Use case scenario: Intelligent RAT Coexistence.

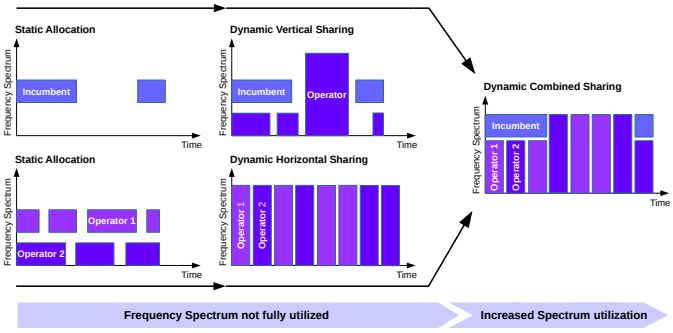

Fig. 14. Use case scenario: Coordinated Spectrum Sharing Schemes.

There exists two main approaches for spectrum sharing, namely, uncoordinated and coordinated. Uncoordinated approaches make use of contention-based mechanisms like the LBT in LTE-LAA and Carrier-sense multiple access with collision avoidance (CSMA/CA) in Wi-Fi. However, at high traffic loads, as users (i.e., radios) are always competing for access to the medium without any cooperative access planning and organization, the number of collisions can be very high, which increases the radios' backoff period and as a consequence, drastically reduces their throughput. Such an approach is far from optimal in terms of spectrum efficiency and QoS guarantees.

On the other hand, coordinated spectrum sharing makes use of a centralized database or spectrum allocation authority, or over-the-air protocols to define a cooperative access planning and organization among users, i.e., radios. The efficiency and robustness of spectrum sharing users can be hugely increased by exploring tight coordination and time synchronization among them. Coordinated sharing has the opportunity to introduce new sharing paradigms such as vertical, horizontal and dynamic (combined) spectrum sharing, as depicted in Figure 14. By analyzing Figure 14, it is clear that a better spectrum utilization can be achieved by a dynamic spectrum sharing coordination among users. The tight coordination of time and frequency resources among users can deliver QoS levels similar to that of users with exclusive allocations of spectrum bandwidth. Through coordinated spectrum sharing, primary users (e.g. incumbents) can get prioritized access to guaranteed resources, while any spectrum not used by primary users can be dynamically allocated between secondary users.

In this use case, the slot-based PHY with its real-time configurable parameters (e.g., Tx PHY BW, transmission timestamp, COT) can be used to devise and assess the performance of new and disruptive sharing protocols and models, deployment scenarios, etc. For example, Game theoretic models can be used to solve spectrum management problems like spectrum trading, spectrum sharing, interference avoidance, power allocation, etc. [71, 72]. In this use case, a central unit, employing a Game theoretic model, would receive requests for time and frequency resource allocation from highly heterogeneous users with different QoS demands and based on some QoS criteria like average throughput, delay, etc. the central unit would try

Preprints (www.preprints.org) | NOT PEER-REVIEWED | Posted: 1 October 2018 doi:10.20944/preprints201810.0017.v1

to maximize the system-wide QoS following some pricing mechanism for resource allocation [72], i.e., the central unit optimizes the spectrum resources in order to meet the users' QoS requirements [73].

VIII. Experiment Results

In this section we present some experimental results in order to demonstrate the effectivenesses and usability of the proposed framework. All the experiments presented here were carried out with the framework running on servers with Intel Core i7-6700 CPUs (@3.40GHz, 8 M cache, 8 GT/s DMI3, Turbo, HT, 4 Cores/8 Threads, 65 Watts) with 128 GB of RAM memory connected to X310 USRPs with 10 Gigabit Ethernet links, and equipped with CBX-120 RF daughterboards [74]. These RF daughterboards operate from 1200 up to 6000 MHz with a bandwidth of 120 MHz [74]. A PHY BW of 5 MHz is selected for the experiments presented in this section, which in frequency corresponds to 25 RBs * 12 subcarriers * 15 KHz (subcarrier separation in frequency domain) = 4.5 MHz.

A. Experiment with Filtered-OFDM waveform

Next we present a few comparison results showing how OOB emissions can be mitigated with the use of a FIR filter added to the PHY Tx processing chain, just after the OFDM symbol modulation. First, we present some results collected at the Rx side of the proposed slot-based PHY.

Figure 15 depicts the comparison of OOB emissions between the OFDM and Filtered-OFDM waveforms at the receiver side of the slot-based PHY for two different FIR filter orders, 64 and 128 respectively. For this result, the FIR filter, either with order 64 or 128, is added to the Tx processing flow (i.e., OFDM symbol modulation), see Figure 7. The figure is obtained by collecting IQ samples at the receiver side of the slot-based PHY, after Rx front end-processing (RF and digital processing) and after the slot (i.e., subframe) is synchronized and aligned, therefore, this is the signal fed into

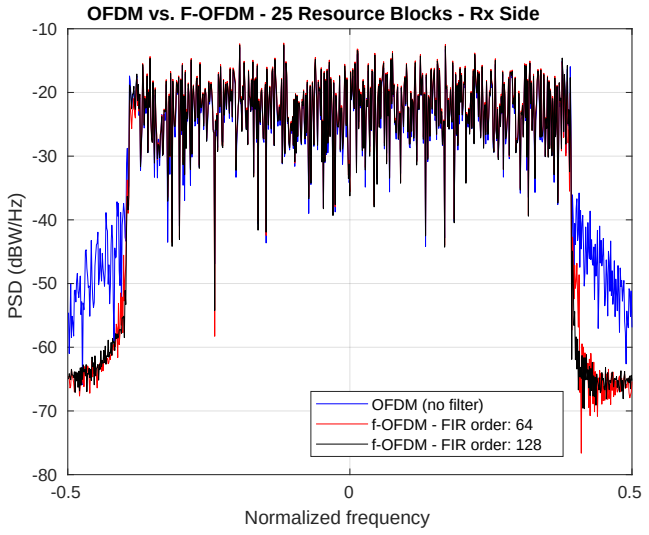

Fig. 15. OFDM and Filtered-OFDM OOB emissions comparison at Rx side.

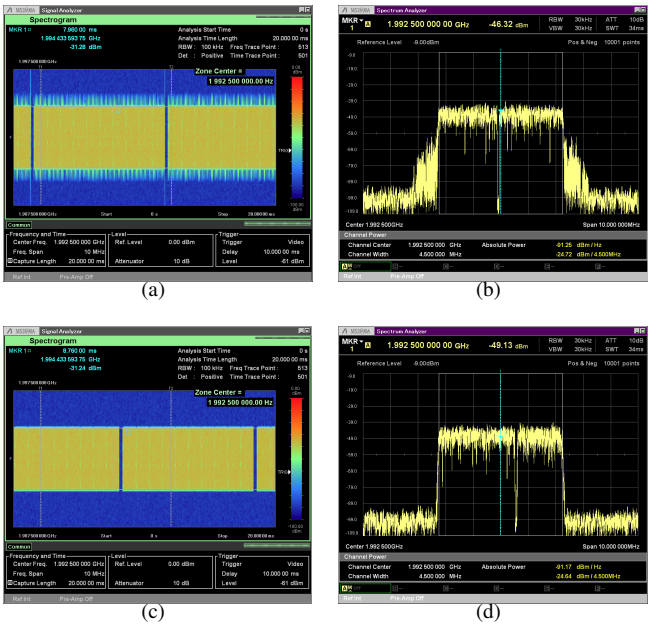

Fig. 16. Comparison between OFDM and Filtered-OFDM. (a) Spectrogram with OFDM (i.e., no filter). (b) Spectrum with no filter enabled. (c) Spectrogram with 128 order FIR filter enabled. (d) Spectrum with 128 order FIR filter enabled.

TABLE VI
OFDM vs. f-OFDM OOB emission and processing time comparison.

FIR order	PSD @ 0.4*fs* [dBW/Hz]	PSD @ 0.5*fs* [dBW/Hz]	Processing time [ms]
No Filter	-40.83	-56.21	-
64	-52.12	-64.52	0.12
128	-55.39	-65	0.24

the demodulation module at the receiver side of the slot-based PHY. Table VI compares some approximate measurements of power spectral density (PSD) and filter processing time.

As can be seen by analyzing Figure 15 and Table VI, the filter reduces the OOB emissions from around -40 dBW/Hz to less than -52 dBW/Hz at the edge of the transmitted signal, around 0.4*fs*, where *fs* is the sampling rate. As can also be noticed in Figure 15, the 128 order FIR filter has, as expected, a sharper transition region when compared to the 64 order FIR filter. Table VI also shows the processing time for each one of the FIR filter orders. The processing time presented in the table considers the time it takes to filter a 1 ms long slot. The values are the result of the average of 10000 slot transmissions. For a PHY with 25 RBs of BW, a 1 ms long slot is composed of 5760 complex samples, i.e., 5760 I/Q samples. Each complex sample is represented by 32 bits (i.e., 4 bytes, with 2 bytes representing each one of the I and Q components), which means the filter has to process 23040 bytes.

In Figure 16 we compare the spectrogram and spectrum of OFDM and f-OFDM transmissions collected with an Anritsu MS2690A Signal Analyzer. The figures were collected with a Tx center frequency of 1.9925 GHz, Tx gain of 3 dB with

Preprints (www.preprints.org) | NOT PEER-REVIEWED | Posted: 1 October 2018 doi:10.20944/preprints201810.0017.v1

TABLE VII

DIFFERENCE BETWEEN P_{ADJ} (NO FILTER) AND P_{ADJ} (64/128 ORDER FILTERS).

Offset	L1 (-5 MHz)		U1 (+5 MHz)		L2 (-10 MHz)		U2 (+10 MHz)		Tx gain
FIR order	64	128	64	128	64	128	64	128	[dB]
Difference [dB]	15.69	15.97	14.82	14.66	0.01	0.16	0.29	0.27	3
	18.5	18.82	17.77	18	0.38	0.6	0.09	0.21	6
	20.43	20.39	19.06	19.17	0.56	0.03	0.20	0.55	9
	21.88	21.27	21.24	20.95	0.51	0.21	0.30	0.49	12
	23.09	22.89	22.47	22.28	0.22	0.02	0.21	0.54	15
	23.11	22.71	22.1	21.84	0.65	0.26	0.47	0.40	18
	22.9	22.59	21.07	20.73	0.48	0.21	0.32	0.13	21
	19.38	18.94	17.52	16.94	0.48	0.14	0.25	-0.02	24
	11.21	10.8	10.51	10.19	0.67	0.36	0.6	0.35	27
	3.29	3.02	2.74	2.51	1.18	0.68	1.12	0.51	30

the USRP Tx output connected to the signal analyzer through a cable with 20 dB of attenuation. It is easily seen that the OFDM side lobes (i.e., OOB emissions) are reduced with the use of the 128 order FIR filter.

The USRP expects to be fed with samples at a rate close to *fs*, however, if the processing time of the Tx chain increases so that it can not deliver samples fast enough (i.e., at a rate close to *fs*), then the USRP starts outputting 'U's (Underflows) at the command line, meaning, that the slot-based PHY transmitter is not supplying samples fast enough. Therefore, in order to keep the Tx processing flow close to the specified sample rate, the processing time of the filter must be as low as possible. During the experiments with the current setup, we also tested higher order filters like 256 and 512, however, the processing time increased to the point where the slot-based PHY transmitter was not being able to supply samples fast enough to the USRP. For smaller PHY BWs the number of complex samples making up a slot is smaller, which makes it possible to use higher order filters. Other FIR filter orders can be easily added to the slot-based PHY by just updating the table with filter coefficients.

Another kind of measurement that was performed in order to show the improvement provided by the f-OFDM waveform is

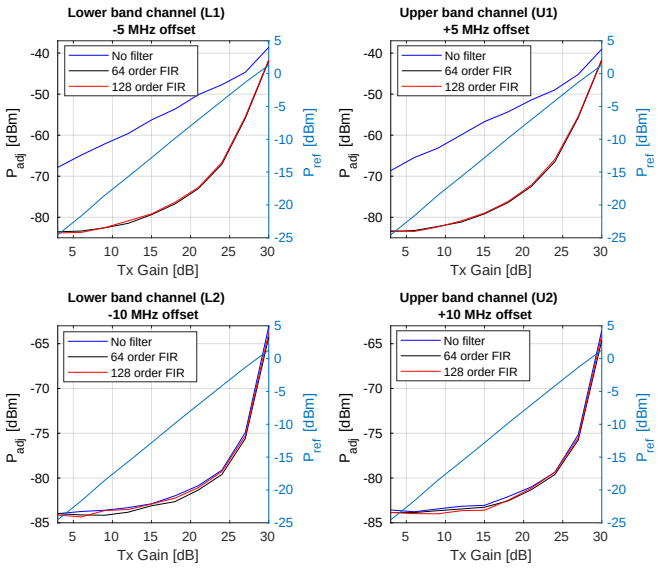

Fig. 17. ACLR measurements for different Tx gains and filter orders.

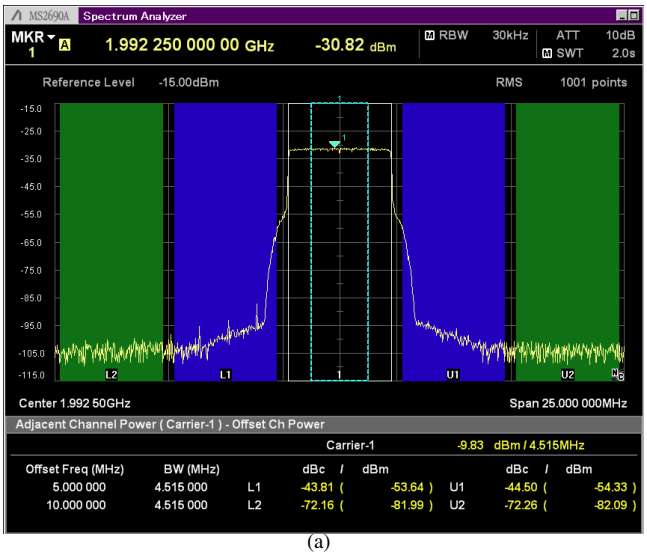

(a)

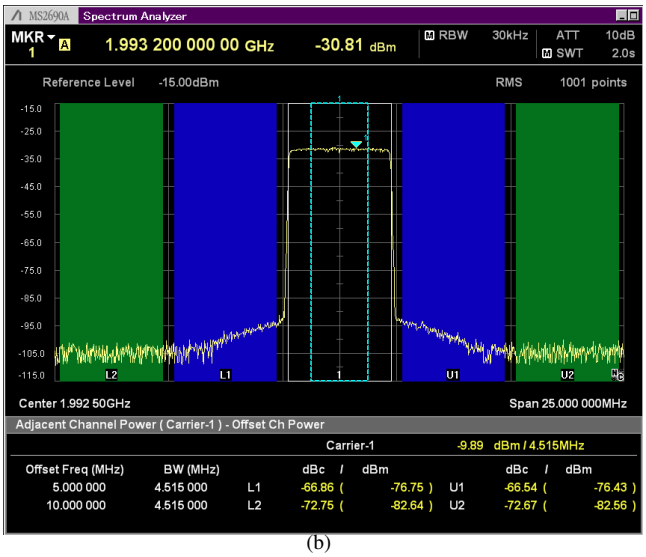

(b)

Fig. 18. ACLR comparison between OFDM and Filtered-OFDM with Tx gain equal to 18 dB. (a) OFDM with no filter enabled. (b) 64 order FIR filter enabled.

known as Adjacent Channel Leakage Ratio (ACLR). ACLR is an important characteristic of wireless transmitters and is defined as an important wireless metric by national laws regulating radio standards as well as by 3GPP and IEEE.

ACLR is defined as the ratio between the total integrated adjacent channel average power, P_{adj}, centered at upper and lower channel frequencies and the total integrated reference channel average power, P_{ref}, centered at the assigned reference channel frequency (i.e., in-band power), where the powers are measured after a receiver filter [75]. The ACLR metric is defined as

$$\text{ACLR(dBc)} = 10\log_{10}\left(\frac{P_{\text{adj}}}{P_{\text{ref}}}\right) = P_{\text{adj}}(\text{dBm}) - P_{\text{ref}}(\text{dBm}). \quad (1)$$

In digital communications systems, the power that leaks

Preprints (www.preprints.org) | NOT PEER-REVIEWED | Posted: 1 October 2018 doi:10.20944/preprints201810.0017.v1

from a transmitted signal into adjacent channels can interfere with transmissions in the neighboring channels and decrease the neighbor system's performance. For LTE, the ACLR metric verifies that transmitters are performing within specified limits defined in the 3GPP specifications [76, 77].

Figure 17 presents the adjacent channel average power, P_{adj} in dBm, for different frequency offsets, Tx gain values and FIR filter orders. The figure also shows the reference channel average power P_{ref} in dBm. The measurements were also taken with the Anritsu MS2690A Signal Analyzer for a setup where Tx center frequency is set to 1.9925 GHz, COT is set to 100 ms, which means 100 1 ms-long slots are transmitted in a row, with an idle time of 1 ms between consecutive transmissions and MCS is set to 0. The Tx gain is changed from 3 up to 30 dB in steps of 3 dB for three different cases: no filter, 64 and 128 order FIR filters. The connection between the USRP and the Spectrum Analyzer is done through cable and attenuation of 20 dB is applied to the signal.

Table VII shows the difference between P_{adj} when no filter is used and P_{adj} when 64 or 128 order FIR filters are used. As can be seen, the power leakage on adjacent channels with frequency offset of +/- 5 MHz is greatly decreased when using any of the two filter orders. For these cases, the leakage reduction can be as high as 23.11 dB for a Tx gain of 18 dB (probably the most linear region of the Tx power amplifier). It can also be noticed that the leakage reduction for both filters orders is quite close. This means that the 64 order filter can be employed without any huge impact on the leakage onto adjacent channels while reducing the Tx flow processing time. On the other hand, the power leakage on adjacent channels with frequency offset of +/- 10 MHz is marginally decreased (at most 1.18 dB reduction), meaning that the leakage level on those channels is already very low even without filter. Figure 18 depicts one example of the ACLR measurement for a Tx gain of 18 dB with OFDM filtering disabled and enabled (64 order FIR filter) respectively. It is easily noticeable that the OFDM skirt is mitigated when the filter is enabled.

All the experiment results presented in this subsection show that the designed filters are able to attenuate out-of-band emissions without affecting in-channel performance.

B. Experiment with the LBT module

In this section we describe the results of an experiment with the LBT module. The main goal of this experiment is to show that LBT can decrease the number of collisions and consequently improve the coexistence among radios operating at the same frequency.

The experiment consists of three different steps. For all the three different steps we want to assess the coexistence performance in terms of CQI and RSSI measurements. The CQI is a quantized version of the signal-to-interference-plus-noise ratio (SINR) measurement that indicates the channel quality. The receiver reports CQI measurements back to the transmitter indicating the data rate supported by the channel at that instant. This measurement report helps the transmitter to choose the optimum modulation and code rate, i.e., MCS, for its transmission. CQI is quantized as shown in [78]. The SINR is calculated as follows

$$\text{SINR} = 10\log_{10}\left(\frac{\text{RSRP}}{\text{noise\_power}_{\text{AVG}}}\right), \tag{2}$$

where RSRP means Reference Signal Received Power and is the linear average of reference signal power across the specified bandwidth (in number of PRBs). When a collision happens, the average noise power increases as the interference being caused by other radios' transmissions is perceived by the receiver as effective noise. Consequently, the SINR decreases, which in turn decreases the CQI. The RSRP is calculated as

$$\text{RSRP} = \frac{\sum_{k=0}^{P-1}|Y_p(k)|^2}{P}, \tag{3}$$

where $Y_p(k)$ represents the received pilot symbol values in the frequency domain, i.e., the value of resource elements (RE) carrying Cell-Specific Reference Signal (CRS) over the entire PHY bandwidth, and $P = 8\ \times$ number of PRBs used by PHY. The average noise power over all REs carrying pilot symbols is estimated as [79, 80]

$$\text{noise\_power}_{\text{AVG}} = \frac{1}{P}\sum_{k=0}^{P-1}|Y_p(k) - \tilde{H}_p(k)X_p(k)|^2, \tag{4}$$

where $X_p(k)$ represents the known transmitted pilot symbol values and $\tilde{H}_p(k)$ is the estimated channel response for the RE occupied by the k-th pilot symbol. The channel response at REs carrying pilot symbols is obtained by dividing the received pilot symbols by their expected values,

$$\tilde{H}_p(k) = \frac{Y_p(k)}{X_p(k)} = H_p(k) + \text{noise}. \tag{5}$$

The other performance metric used in the experiment is the RSSI. It measures the average total received power observed over the whole slot (i.e., 1 ms) duration. The RSSI is calculated as

$$\text{RSSI} = 10\log_{10}\left(\frac{\sum_{n=0}^{N-1}|y(n)|^2}{N}\right), \tag{6}$$

where $y(n)$ is the received slot signal in time domain, N is the slot size in number of complex samples, which is, for example, equal to 5760 samples for a 5 MHz PHY. When a collision happens, the transmitted signals (i.e., slots) overlap and consequently, the measured RSSI will be higher as the received signal is the combination of several transmissions that happen at the same time and frequency.

For all the three steps of this experiment we used a testbed that provides a constant 60 dB path loss for all radio pairs and

TABLE VIII
LBT EXPERIMENT MEASUREMENTS.

Step	CQI		RSSI		Collision
	Mean	Variance	Mean	Variance	%
Simplex	14.77	0.37	-25.33	0.0003	0
LBT Disabled	12.79	11.02	-25.10	0.2258	31.813
LBT Enabled	13.78	1.27	-25.24	0.0091	0.038

Preprints (www.preprints.org) | NOT PEER-REVIEWED | Posted: 1 October 2018 doi:10.20944/preprints201810.0017.v1

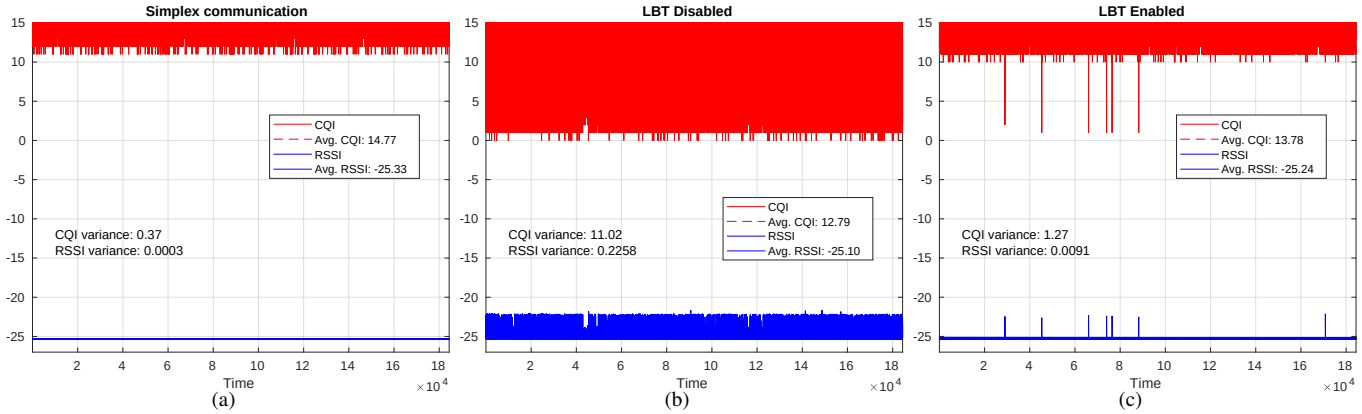

Fig. 19. Comparison when LBT is disabled and enabled. (a) Simplex operation: one radio transmits and the other one only receives. (b) Two radios transmitting on the same channel without any contention mechanism. (c) Two radios transmitting on the same channel with LBT enabled.

a bandwidth of 6 MHz, i.e., transmitted signals with bandwidth wider than 6 MHz are attenuated. The radios' Tx and Rx gains are set to 20 dB, COT is set to 25 ms, i.e., 25 slots are transmitted in sequence without any gap between subsequent slots, and the idle time is set to 10 ms, i.e., the interval between COTs. We transmitted more than 180×10^3 slots with MCS equal to 0 for each step of the experiment.

For the first step, we assess the performance when there is no collision involved. In this step there are two radios working in simplex mode, i.e., one radio transmits and the other one only receives. In this step there are no collisions. As can be seen in Figure 19 (a), RSSI is constant at around 25 dBW and CQI varies between 11 and 15 throughout the trial.

In the second step, we want to assess the performance when two radios compete for access to the medium (i.e., two radios operating in full-duplex mode at the same central frequency) without any contention mechanism. Figure 19 (b) shows that RSSI is not constant anymore, varying between -25 and -21 dBW while CQI varies between 0 and 15 throughout the trial. The fluctuation in both CQI and RSSI values are due to collisions. As a way to estimate the number of collisions during the step, we count as a collision CQI measurements with value less than 11, which is the minimum CQI value for the simplex communication case, where no collisions happen. By using this approach, the percentage of collisions is equal to 31.813 %.

The third step is similar to the second step with the only difference being the use of a contention mechanism, i.e., LBT. In this step we assess the performance when LBT is enabled with a threshold of -70 dBW, CCA of 173.26 μs and a random backoff of at most 32 CCA intervals. Figure 19 (c) shows that RSSI is much more constant, staying around -25 dBW with very few points where it goes to -21 dBW. The CQI behavior is also closer to that depicted in (a), with CQI varying between 10 and 15 and very few points where it drops to 0 throughout the trial. The percentage of collisions is equal to 0.038 % using the same approach described earlier to estimate the number of collisions. Table VIII summarizes the results of the three steps of the experiment.

Based on the results of this experiment, it is clearly seen that either CQI or RSSI measurements (or even both of them) could be used as an approach to detect collisions. For example, these measurements could be employed in LTE systems to detect collisions more effectively in a timely manner and consequently, decrease the inherent latency of those systems. In LTE systems, due to the inherent latencies introduced by the LTE protocol stack, the HARQ feedback associated to a certain subframe is received at least 4 ms after its transmission time [81].

C. Experiment with MF-TDMA feature

In this section we show the capability of the slot-based PHY to work in MF-TDMA mode with the use of the transmission timestamp field in the Tx control message. MF-TDMA is a two-dimensional multiple access scheme that combines frequency division with time division access to the medium. Due to its efficiency and flexibility, MF-TDMA scheme has been widely used in several communications systems such as very small aperture terminal (VSAT) satellite communications systems [82]. A MF-TDMA communications system is composed of several channels, where each one of the channels is divided into a number of time slots. Such scheme ensures adaptability and improves the radio resources utilization for multi-user and multi-service applications [82].

Figure 20 shows two spectrograms collected during 40 ms over a 31.25 MHz bandwidth with the slot-based PHY set to operate with 6 channels with a channel spacing of 2.5 MHz. In this experiment, one radio transmits a random number of slots at randomly selected channels. The channel number and number of transmitted slots, i.e., COT, are randomly selected between the ranges 0-5 and 1-3 respectively.

Figure 20 (a) presents the spectrogram for the case with no filtering enabled (i.e., OFDM waveform) and with a gap of 1 ms between consecutive transmissions. As can be noticed, with the current channel spacing, the OFDM OOB emissions might interference with adjacent channels and consequently decrease the system's throughput. The OOB emissions can be mitigated with the use of filtering.

Preprints (www.preprints.org) | NOT PEER-REVIEWED | Posted: 1 October 2018 doi:10.20944/preprints201810.0017.v1

Figure 20 (b) depicts the spectrogram for the case when the filtered-OFDM waveform is enabled with a gap of 0.5 ms between consecutive transmissions. As can be seen, when the filtered-OFDM is used, the OOB emissions are mitigated and consequently, interference with and from adjacent channels is also mitigated or completely eliminated. Additionally, another consequence of the filtering is that the channel spacing could be made smaller and consequently improving the radio resource utilization.

D. slot-based PHY Profiling

In this section we present some measurements regarding the average Tx and Rx processing times of the proposed slot-based PHY. Table IX shows the average processing times for PHY BWs of 1.4, 5 and 10 MHz for MCS values of 0, 10 and 18, which use QPSK, 16QAM and 64QAM modulations respectively. The processing times were averaged over 10000 transmissions with COT set to 1 ms, i.e., only 1 slot for each new transmission. For these measurements we set both Tx and Rx gains to 20 dB so that the received signal quality (i.e., SNR) would be good enough for the PHY to reach high MCS values. The Modulation, *Mod.*, column lists the average time it takes to process control/data bits (i.e., channel coding, rate matching, scrambling, modulation, precoding and resource grid mapping) and generate a 1 ms long slot. The Filter column shows the average filtering time. As can be seen, for a given PHY BW, the filtering time is approximately constant. It shows that the filtering time does not depend on the MCS being used as, for a given PHY BW, a slot always has the same size irrespective of the MCS. The Synchronization, *Synch.*, column shows the average time it takes to correlate the received signal with the local PSS sequence, decode the SSS signal, estimate CFO, align the subframe to the buffer start (read from the USRP missing samples necessary to have a full slot in the buffer), and correct CFO. As seen from the table, the synchronization time is approximately constant for a given PHY BW, showing, as expected, that it does not depend on the MCS value. The synchronization time depends only on slot size, i.e., number of I/Q samples making up a slot. The Demodulation, *Demod.*, column lists the average time it takes for the already synchronized slot to be demodulated. As expected, the higher the MCS the higher the decoding time. That is due to the fact that the the information (data) carried by one slot is higher for high MCS values, and therefore, the processing time is longer. Another point that is also worth mentioning is that the demodulation process is the most time-consuming task carried out by PHY.

TABLE IX
AVERAGE TX AND RX PROCESSING TIMES FOR DIFFERENT PHY BWS AND MCS VALUES WITH 64 ORDER FIR FILTER.

PHY BW: 1.4 MHz slot size: 1920 I/Q samples						
MCS	Tx processing time [ms]			Rx processing time [ms]		
	Mod.	Filter	Total	Synch.	Demod.	Total
0 (QPSK)	0.030	0.049	0.079	0.051	0.114	0.165
10 (16QAM)	0.052	0.047	0.099	0.052	0.124	0.176
18 (64QAM)	0.053	0.048	0.101	0.049	0.140	0.189

PHY BW: 5 MHz slot size: 5760 I/Q samples						
MCS	Tx processing time [ms]			Rx processing time [ms]		
	Mod.	Filter	Total	Synch.	Demod.	Total
0 (QPSK)	0.072	0.120	0.192	0.185	0.166	0.351
10 (16QAM)	0.101	0.122	0.223	0.185	0.212	0.397
18 (64QAM)	0.135	0.120	0.255	0.187	0.284	0.471

PHY BW: 10 MHz slot size: 11520 I/Q samples						
MCS	Tx processing time [ms]			Rx processing time [ms]		
	Mod.	Filter	Total	Synch.	Demod.	Total
0 (QPSK)	0.134	0.285	0.419	0.383	0.283	0.666
10 (16QAM)	0.175	0.283	0.458	0.384	0.407	0.791
18 (64QAM)	0.256	0.287	0.543	0.382	0.543	0.925

IX. CONCLUSIONS AND FUTURE WORK

This paper presented a open source SDR-based framework that enables experimental research and prototyping for various next generation wireless networks spectrum sharing scenarios. Its high configurability, supported by an interface built upon popular programming libraries (Google protobuf and ZeroMQ), allows engineers and researchers to easily modify it or extend its functions by plugging in new modules implementing novel spectrum sharing techniques and approaches. Additionally, the proposed slot-based PHY is of great importance to combat spectrum scarcity as it has a pivotal role in providing optimum utilization of time-frequency resources. These features make it the perfect candidate for an extensive range of spectrum sharing experimentations in real-world or realistic environments such as testbeds aiming at better understanding disruptive spectrum sharing schemes. Three distinctive use cases are presented with hints on how the proposed framework could be employed in intelligent spectrum sharing research.

As future work, we aim at adding support to self-contained slots and scalable OFDM-based air interface. With self-contained slots, both data and acknowledgement (ACK) information are present in the same time slot. This feature allows each transmission to be a modular transaction, giving PHY the ability to independently decode slots and avoid static timing relationships across slots like in LTE systems. Moreover, self-contained slots are a key enabler to low latency. With a scalable air interface numerology, parameters like subcarrier spacing and transmission time interval (TTI) can be dynamically and efficiently modified to support the diverse frequency, channel bandwidths, deployments, and services foreseen to exist in next generation mobile networks. Additionally, we also plan to offload a few time-consuming PHY processing tasks (e.g., slot synchronization, FIR filtering, OFDM modulation and demodulation) to the FPGA as a way to increase both real-time and processing performance.

ACKNOWLEDGEMENTS

The project leading to this publication has received funding from the European Union's Horizon 2020 research and inno-

Preprints (www.preprints.org) | NOT PEER-REVIEWED | Posted: 1 October 2018 doi:10.20944/preprints201810.0017.v1

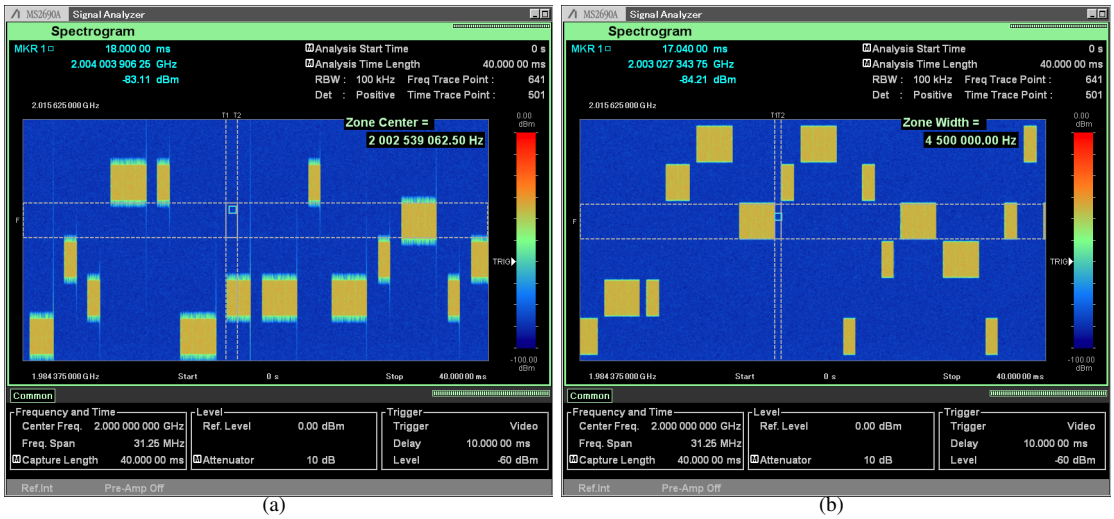

Fig. 20. Comparison of MF-TDMA feature without and with filtering. (a) OFDM without filtering. (b) 128 order FIR filter enabled.

vation programme under grant agreement No. 732174 (ORCA project).

REFERENCES

[1] Cisco, *Cisco Visual Networking Index: Global Mobile Data Traffic Forecast Update, 2015-2020*, White paper, February 2016.

[2] The 5G Infrastructure Public Private Partnership (5G-PPP) Technical Report, *5G empowering vertical industries*, February 2016.

[3] 3GPP Technical Report TR 38.913, *Study on scenarios and requirements for next generation access technologies, version 14.2.0, Release 14*, March 2017.

[4] Michael Koziol, *5G New Radio and What Comes Next*, IEEE Spectrum, January 2018.

[5] Gregory Staple and Kevin Werbach, *The End of Spectrum Scarcity*, IEEE Spectrum, March 2014.

[6] Recommendation ITU-R M.2083, *IMT Vision - Framework and overall objectives of the future development of IMT for 2020 and beyond*, September 2015.

[7] ITU-R Report M.2370-0, *IMT traffic estimates for the years 2020 to 2030*, July 2015.

[8] Keith Mallinson, *The path to 5G: as much evolution as revolution*, May 2016. [available at] http://www.3gpp.org/news-events/3gpp-news/1774-5g_wiseharbour.

[9] Oumer Teyeb, Gustav Wikstrom, Magnus Stattin, Thomas Cheng, Sebastian Faxer, and Hieu Do, *Evolving LTE to fit the 5G future*, Ericsson Technology Review, January 2017. [available at] https://www.ericsson.com/en/ericsson-technology-review/archive/2017/evolving-lte-to-fit-the-5g-future

[10] Konstantinos Chatzikokolakis, Panagiotis Spapis, Alexandros Kaloxylos, and Nancy Alonistioti, *Toward spectrum sharing: opportunities and technical enablers*, IEEE Communications Magazine, vol. 53, no. 7, July 2015.

[11] Junyu Liu, Min Sheng, Lei Liu, and Jiandong Li, *Network Densification in 5G: From the Short-Range Communications Perspective*, IEEE Communications Magazine, vol. 55, no. 12, December 2017.

[12] Yan Li, and Shaoyi Xu, *Traffic Offloading in Unlicensed Spectrum for 5G Cellular Network: A Two-Layer Game Approach*, MDPI Entropy, January 2018.

[13] Federal Communications Commission, *Spectrum Policy Task Force Report*, [available online] https://www.fcc.gov/document/spectrum-policy-task-force, FCC, November 2002.

[14] Andreas Roessler, *Impact of spectrum sharing on 4G and 5G standards a review of how coexistence and spectrum sharing is shaping 3GPP standards*, IEEE International Symposium on Electromagnetic Compatibility & Signal/Power Integrity (EMCSI), October 2017.

[15] Mina Labib, Vuk Marojevic, Jeffrey H. Reed, and Amir I. Zaghloul, *Extending LTE into the Unlicensed Spectrum: Technical Analysis of the Proposed Variants*, IEEE Communications Standards Magazine, vol. 1, no. 4, December 2017.

[16] Qualcomm Technologies, Inc., *LTE-U/LAA, MuLTEfire and Wi-Fi; making best use of unlicensed spectrum*, White Paper, September 2015.

[17] MulteFire Alliance, *MulteFire Release 1.0 Technical Paper: A new way to wireless*, January 2017.

[18] Ahsan Saadat, Gengfa Fang, and Wei Ni, *A Two-Tier Evolutionary Game Theoretic Approach to Dynamic Spectrum Sharing through Licensed Shared Access*, IEEE International Conference on Computer and Information Technology; Ubiquitous Computing and Communications; Dependable, Autonomic and Secure Computing; Pervasive Intelligence and Computing, October 2015.

[19] Nadine Abbas, Youssef Nasser, and Karim El Ahmad, *Recent advances on artificial intelligence and learning techniques in cognitive radio networks*, EURASIP Journal on Wireless Communications and Networking, vol. 2015, no. 1, pp. 174-194, December 2015.

[20] Seppo Yrjola, and Heikki Kokkinen, *Licensed Shared Access evolution enables early access to 5G spectrum and novel use cases*, EAI Endorsed Transactions on Wireless Spectrum, December 2017.

[21] J. Mitola, *The software radio architecture*, IEEE Communications Magazine, vol. 33, no. 5, May 1995.

[22] J. Mitola, *Software radios-survey, critical evaluation and future directions*, National Telesystems Conference (NTC), May 1992.

[23] Felipe A. P. de Figueiredo, *A Framework for Intelligent Spectrum Sensing and Sharing*, [online] Available: https://github.com/zz4fap/intelligent-spectrum-sharing, May 2018.

[24] Ettus Research LLC, *USRP Hardware Driver*, [online] Available: http://files.ettus.com/manual/

[25] Ettus Research LLC, *Products*, [online] Available: https://www.ettus.com/product

[26] *Open Air Interface*, 2015. [Online]. Available: http://www.openairinterface.org/

[27] *openLTE*, 2015. [Online]. Available: http://openlte.sourceforge.net/

[28] I. Gomez-Miguelez, A. Garcia-Saavedra, P. D. Sutton, P. Serrano, C. Cano and D. J. Leith, *srsLTE: An Open-Source Platform for LTE Evolution and Experimentation*, ACM WiNTECH Workshop, October 2016.

[29] Amarisoft Corp. *Amari LTE 100 - Software LTE base station on PC*, [Available online] http://www.amarisoft.com

[30] National Instruments, *LabVIEW Communications LTE Application Framework 2.0 and 2.0.1*, White Paper, December 2016. [Online]. Available: http://www.ni.com/white-paper/53286/en/

[31] National Instruments, *Real-time LTE/Wi-Fi Coexistence Testbed*, White Paper, February 2016. [Online]. Available: http://www.ni.com/white-paper/53044/en/

[32] Zhenyu Zhou, Yunjian Jia, Fei Chen, Kimfung Tsang, Guangyi Liu, and Zhu Han, *Unlicensed Spectrum Sharing: From Coexistence to Convergence*, IEEE Wireless Communications, vol. 24, no. 5, October 2017.

[33] Cristina Cano, Douglas J. Leith, Andres Garcia-Saavedra, and Pablo Serrano, *Fair Coexistence of Scheduled and Random Access Wireless Networks: Unlicensed LTE/Wi-Fi*, IEEE/ACM Transactions on Networking, vol. 25, no. 6, December 2017.

[34] D. Ruby, M. Vijayalakshmi, and A. Kannan, *Intelligent relay selection and spectrum sharing techniques for cognitive radio networks*, Cluster Computing, August 2017.

[35] Usama Mir, Leila Merghem-Boulahia, Dominique Gaiti, *Dynamic Spectrum Sharing in Cognitive Radio Networks: a Solution based on Multiagent Systems*, International Journal on Advances in Telecommunications, vol. 3 no. 3, January 2010.

[36] Nadisanka Rupasinghe, and Ismail Guvenc, *Reinforcement learning for licensed-assisted access of LTE in the unlicensed spectrum*, IEEE Wireless Communications and Networking Conference (WCNC), June 2015.

[37] Ruben Mennes, Miguel Camelo, Maxim Claeys and Steven Latre, *A Neural-Network-based MF-TDMA MAC Scheduler for Collaborative Wireless Networks*, IEEE Wireless Communications and Networking Conference (WCNC), April 2018.

[38] Zoraze Ali, Lorenza Giupponi, Josep Mangues-Bafalluy, and Biljana Bojovic, *Machine learning based scheme for contention window size adaptation in LTE-LAA*, IEEE Annual International Symposium on Personal, Indoor, and Mobile Radio Communications (PIMRC), February 2018.

[39] P. Hintjens, *ZeroMQ Messaging for Many Applications*, O'Reilly Media, March 2013.

[40] Ettus Research LLC, *USRP X Series*, [Online] Available: https://www.ettus.com/product/category/USRP-X-Series

[41] National Instruments, *Overview of the NI USRP RIO Software Defined Radio*, White Paper, December 2015. [Online]. Available: http://www.ni.com/white-paper/52119/en/

[42] Google, *protobuf - Protocol Buffers - Google's data interchange format*, [online], Available: http://code.google.com/p/protobuf/, 2011.

[43] DARPA SC2 Website: https://spectrumcollaborationchallenge.com/.

[44] DAPRA, *Kick-off meeting*, The Johns Hopkins University, January 2017.

[45] Cristina Cano, and Douglas J. Leith, *Unlicensed LTE/Wi-Fi coexistence: Is LBT inherently fairer than CSAT?*, IEEE International Conference on Communications (ICC), July 2016.

[46] Houman Zarrinkoub, *Overview of the LTE Physical Layer*, John Wiley & Sons, January 2014.

[47] Sravanthi Kanchi, Shubhrika Sandilya, Deesha Bhosale, Adwait Pitkar, and Mayur Gondhalekar, *Overview of LTE-A technology*, IEEE Global High Tech Congress on Electronics (GHTCE), March 2014.

[48] Shao-Yu Lien, Shin-Lin Shieh, Yenming Huang, Borching Su, Yung-Lin Hsu, and Hung-Yu Wei, *5G New Radio: Waveform, Frame Structure, Multiple Access, and Initial Access*, IEEE Communications Magazine, vol. 55, no. 6, June 2017.

[49] Naga Bhushan, Tingfang Ji, Ozge Koymen, John Smee, Joseph Soriaga, Sundar Subramanian, and Yongbin Wei, *5G Air Interface System Design Principles*, IEEE Wireless Communications, October 2017.

[50] ANSI/IEEE 802.11n-2009 , *IEEE Standard for Information technology - Local and metropolitan area networks - Specific requirements - Part 11: Wireless LAN Medium Access Control (MAC)and Physical Layer (PHY) Specifications Amendment 5: Enhancements for Higher Throughput*, 2010.

[51] ETSI TR 101.190, *Digital Video Broadcasting (DVB); Framing structure, channel coding and modulation for digital terrestrial television - V1.6.1*, January 2009.

[52] Gwanmo Ku, and John MacLaren Walsh, *Resource Allocation and Link Adaptation in LTE and LTE Advanced: A Tutorial*, IEEE Communications Surveys & Tutorials, vol. 17, no. 3, December 2014.

[53] 3GPP TS 36.213, *Physical Layer Procedures*, 3rd Generation Partnership Project; Technical Specification Group Radio Access Network; Evolved Universal Terrestrial Radio Access (E-UTRA). URL: http://www.3gpp.org, May 2016.

[54] Quentin Bodinier, Faouzi Bader, and Jacques Palicot, *On Spectral Coexistence of CP-OFDM and FB-MC Waveforms in 5G Networks*, IEEE Access, vol. 5, July 2017.

[55] Hao Lin, and Pierre Siohan, *Major 5G Waveform Candidates: Overview and Comparison*, Book chapter in Signal Processing for 5G, Wiley, August 2016.

[56] Lei Zhang, Ayesha Ijaz, Pei Xiao, Mehdi M. Molu, and Rahim Tafazolli, emphFiltered OFDM Systems, Algorithms, and Performance Analysis for 5G and Beyond, IEEE Transactions on Communications, vol. 66, no. 3, March 2018.

[57] Javad Abdoli, Ming Jia, and Jianglei Ma, *Filtered OFDM: A New Waveform for Future Wireless Systems*, IEEE International Workshop on Signal Processing Advances in Wireless Communications (SPAWC), August 2015.

[58] Xi Zhang, Ming Jia, Lei Chen, Jianglei Ma, and Jing Qiu, *Filtered-OFDM - Enabler for Flexible Waveform in the 5th Generation Cellular Networks*, IEEE Global Communications Conference (GLOBECOM), December 2015.

[59] Felipe A. P. de Figueiredo, Fabbryccio A. C. M. Cardoso, Jose A. Bianco F., Rafael M. Vilela, Karlo G. Lenzi, *Multi-stage Based Cross-Correlation Peak Detection for LTE Random Access Preambles*, Revista Telecomunicacoes, vol. 15, September 2013.

[60] Janne J. Lehtomaki, Johanna Vartiainen, Markku Juntti and Harri Saarnisaari, *Spectrum sensing with forward methods*, in Proc. IEEE Military Commun. Conf., pp. 1-7, Washington, D.C., USA, October 2006.

[61] Gen Li, Tan Wang, Qingyu Miao, Ying Wang, and Biao Huang, *Spectrum Sharing for 5G*, 5G Mobile Communications, Springer, Cham, October 2016.

[62] X. Wang et al., *Throughput and Fairness Analysis of Wi-Fi and LTE-U in Unlicensed Band*, IEEE JSAC, vol. 35, no. 1, pp. 63-78, January 2017.

[63] 3GPP TR 36.889, *Feasibility Study on Licensed-Assisted Access to Unlicensed Spectrum (Release 13)*, January 2015.

[64] Mina Labib, Vuk Marojevic, Jeffrey H. Reed, and Amir I. Zaghloul, *Extending LTE into the Unlicensed Spectrum: Technical Analysis of the Proposed Variants*, IEEE Communications Standards Magazine, vol. 1, no. 4, December 2017.

[65] Jaehong Yi, Weiping Sun, Seungkeun Park, and Sunghyun Choi, *Performance Analysis of LTE-LAA Network*, IEEE Communications Letters, December 2017.

[66] Xianjun Jiao, Ingrid Moerman, Wei Liu, and Felipe A. P. de Figueiredo, *Radio Hardware Virtualization for Coping with Dynamic Heterogeneous Wireless Environments*, International Conference on Cognitive Radio Oriented Wireless Networks (CROWNCOM), September 2017.

[67] Vasilis Maglogiannis, Dries Naudts, Adnan Shahid, and Ingrid Moerman, *An adaptive LTE listen-before-talk scheme towards a fair coexistence with Wi-Fi in unlicensed spectrum*, Telecommunication Systems, January 2018.

[68] Anand M. Baswade, and Bheemarjuna Reddy Tamma, *Channel sensing based dynamic adjustment of contention window in LAA-LTE networks*, International Conference on Communication Systems and Networks (COMSNETS), March 2016.

[69] Qualcomm Technologies, Inc., *What can we do with 5G NR Spectrum Sharing that isn't possible today?*, White Paper, December 2017.

[70] Ericsson AB, *Spectrum sharing* White Paper, October 2013.

[71] Hai-Yan Shi, Wan-Liang Wang, Ngai-Ming Kwok, and Sheng-Yong Chen, *Game Theory for Wireless Sensor Networks: A Survey*, MDPI Sensors, vol. 12, no. 7, July 2012.

[72] Saed Alrabaee, Mahmoud Khasawneh, Anjali Agarwal, Nishith Goel, and Marzia Zaman, *A game theory approach: Dynamic behaviours for spectrum management in cognitive radio network*, IEEE Globecom Workshops (GC Wkshps), December 2012.

[73] Prabodini Semasinghe, Setareh Maghsudi, and Ekram Hossain, *Game Theoretic Mechanisms for Resource Management in Massive Wireless IoT Systems*, IEE Communications Magazine, vol. 55, no. 2, February 2017.

[74] Ettus Research LLC, *CBX 1200-6000 MHz Rx/Tx (120 MHz, X Series only)*, [online] Available: https://www.ettus.com/product/details/CBX120

[75] 3GPP TS 36.104, *Base Station (BS) radio transmission and reception - V14.3.0*, 3rd Generation Partnership Project; Technical Specification Group Radio Access Network; Evolved Universal Terrestrial Radio Access (E-UTRA). URL: http://www.3gpp.org, April 2017.

[76] 3GPP TS 36.141, *Base Station (BS) Conformance Testing - V8.4.0*, 3rd Generation Partnership Project; Technical Specification Group Radio Access Network; Evolved Universal Terrestrial Radio Access (E-UTRA). URL: http://www.3gpp.org, September 2009.

 doi:10.20944/preprints201810.0017.v1

[77] 3GPP TS 36.521-1, *User Equipment (UE) Conformance Specification; Radio Transmission and Reception Part 1: Conformance Testing - V8.3.1*, 3rd Generation Partnership Project; Technical Specification Group Radio Access Network; Evolved Universal Terrestrial Radio Access (E-UTRA). URL: http://www.3gpp.org, September 2009.

[78] Mohammad T. Kawser, Nafiz Imtiaz Bin Hamid, Md. Nayeemul Hasan, M. Shah Alam, and M. Musfiqur Rahman, *Downlink SNR to CQI Mapping for Different Multiple Antenna Techniques in LTE*, International Journal of Information and Electronics Engineering, vol. 2, no. 5, September 2012.

[79] 3GPP TS 36.141. *Base Station (BS) conformance testing*, 3rd Generation Partnership Project; Technical Specification Group Radio Access Network; Evolved Universal Terrestrial Radio Access (E-UTRA). URL: http://www.3gpp.org.

[80] Van de Beek, J. J., O. Edfors, M. Sandell, S. K. Wilson, and P. O. Borjesson, *On Channel Estimation in OFDM Systems*, IEEE Vehicular Technology Conference, vol. 2, 1995.

[81] Kazuki Takeda, Li Hui Wang, and Satoshi Nagata, *Latency reduction towards 5G*, IEEE Wireless Communications, vol. 24, no. 3, pp. 2-4, June 2017.

[82] D. Qijia, Z. Jun, Z. Tao, and Q. Yong, *Resource Allocation Strategies in MF-TDMA Satellite Systems*, Acta Aeronautica Et Astronautica Sinica, vol. 30 no. 9, pp. 1718-1726, September 2009.